

UNCLASSIFIED

AD NUMBER	
AD011687	
CLASSIFICATION CHANGES	
TO:	unclassified
FROM:	secret
LIMITATION CHANGES	
TO:	Approved for public release, distribution unlimited
FROM:	Distribution authorized to U.S. Gov't. agencies and their contractors; Foreign Government Information; APR 1953. Other requests shall be referred to The British Embassy, 3100 Massachusetts Avenue, NW, Washington, DC 20008.
AUTHORITY	
RARDE List dtd 31 Mar 1966; DSTL, DEFE 15/1818, 27 Oct 2008	

THIS PAGE IS UNCLASSIFIED

Reproduced by

Armed Services Technical Information Age

DOCUMENT SERVICE CENTER

KNOTT BUILDING, DAYTON, 2, OHIO

AD -

1 1 6 8 7

SECRET

13/53

SECRET

COPY No. 83

AD No. 11687

ASTIA FILE COPY



MINISTRY OF SUPPLY

ARMAMENT RESEARCH ESTABLISHMENT

REPORT 13/53

APPLIED RESEARCH DIVISION

A Study of the Mechanism of Scabbing of
Steel Plates by Explosive Attack

R. F. Wilkinson

E. de L. Costello

SECRET

Ministry of Supply

ADVANCED RESEARCH ESTABLISHMENT

REPORT 13/53

A Study of the Mechanism of Scabbing of Steel
Plates by Explosive Attack.

R.P. Wilkinson and E. de L. Costello

Summary

Plates of mild steel have been subjected to attack by cylinders of plastic explosive and the dimensions of the resulting craters and scabs have been determined. The time of arrival of the detonation wave at one surface, and the displacement-time curve over the first 0.2 in. for the other surface, have also been found. From the measurements the variation of pressure at the shock front with distance travelled through the steel has been determined, and values for the shock wave velocity at different pressures have been obtained. The results are in substantial agreement with those predicted theoretically. Previous work relevant to the subject has been examined and the various factors influencing the scabbing phenomenon have been discussed. In the light of both this discussion and the results of the present work, the dependence of the shape of the stress wave on the charge dimensions and the distance travelled has been qualitatively determined; the effect of both charge and plate dimensions on the dimensions of the scab formed has been accounted for.

SECRET

IMPORTANT

This DOCUMENT should be returned to the Chief Information Officer, Armament Research Establishment, Fort Halstead, Sevenoaks, Kent, if retention becomes no longer necessary

INITIAL DISTRIBUTION

Internal

No. 1	CSAR
2	SSAR
3	SSWR
4	SSAM
5	SSAM (Attention Mr.C.K.Thornhill)
6 - 7	SAE
8	SEMP
9	SEPM
10 - 13	SAE (Attention Mr.R.F.Wilkinson, Mr.H.C.James Dr.W.E.Soper, Mr.E. de L.Castello)

United Kingdom

14 - 15	CS/ERDE
16	CS/HER
17	DWR(D)
18	FLER(D)
19	CEAD
20 - 21	CEAD (Attention Lt.Col.Greenway, Major Reader)
22	FWIE
23 - 24	HC of S, Shrivenham
25	Sec.OS
26 - 55	High Explosives Committee (Secretary Mr.R.F.Wilkinson)
56 - 80	Rate of Strain Panel (Secretary Mr.S.J.Tupper)

Overseas (through TRAJ/TIS)

81 - 98	US - Joint Reading Panel
99	- R & D Board
100	- NOTS, Inyokern (Attention Mr.J.S.Rinchart)
101	- NOL, Silver Springs, Md. (attention Dr.J.H.Habland)
102 - 103	DSM (incl. Naval Staff) for own use only
104	Canada - Dept. Nat. Def.
105 - 108	- Def. Res. Liaison
109	- Nat. Res. Council
110	- Canadian Defence Research Board
111 - 112	TRAJ/TIS - Retention

Stock

113 - 128

<u>CONTENTS</u>	<u>PAGE No.</u>
1. Introduction	1
2. Review of previous work	1
3. Experimental Methods	7
3.1 Recording technique	7
3.2 The Charges	8
3.3 The event systems	9
4. Experimental results	10
5. Discussion of results	13
6. Conclusions	21
7. Bibliography	22

Figures 1 to 26

Plates I to III

SECRET

1. Introduction

It is well known that, when a slab of explosive is detonated in contact with a steel plate, the surface of the plate remote from the explosive is scabbed; that is, a fracture occurs near to the free surface parallel with the surface and a piece of metal may be detached. In this country the term scabbing is restricted to those cases where the piece of metal is actually detached, but in the United States the term also includes those cases in which only the fracture parallel to the surface occurs.

This effect has been made use of in the squash-head projectile designed for the defeat of tank armour. This weapon consists of a relatively thin-nosed shell filled with plastic explosive or RDX-wax and base-fused. On impact with the target the nose of the shell collapses and the explosive flows into a slab of diameter greater than that of the original shell. At a suitable instant the fuse initiates the explosive from behind. A large number of firing trials have been carried out in this country (1, 2) and also in the United States and a lot of rather empirical information has been collected together concerning the explosive and scab dimensions.

The work described in this report was undertaken in an attempt to throw some light on the basic mechanism of the scabbing process. A more complete understanding of this may enable improvements to be made in the weapon or, at least, enable the limitations of the weapon to be appreciated. In the work cylindrical charges of plastic explosive were detonated in contact with mild steel plate and attempts were made to measure the scab dimensions, the shock wave velocity through the plate, and the displacement-time curve of the free surface.

2. Review of Previous Work

The effect of the transmission of a transient compressional wave through metal was first studied by Hopkinson (3) and later by Landon (4) and Davies (5). Hopkinson studied the effect produced by the impact of a bullet on a cylindrical steel bar by a method which is still extensively used. Consider a cylinder of material divided into two parts, A and B (fig. 1a), and subjected to a pressure pulse as shown. When the compression wave reaches the free surface it is reflected as a tension wave of equal magnitude (fig. 1b) in order to satisfy the boundary conditions that the pressure at the free surface should remain unchanged. When the reflected tension wave reaches the boundary of the pieces, $x - x$, the joint has no strength in tension and the two parts fly apart. If the thickness of B is greater than half the wavelength of the pulse, all the momentum will be trapped in it and this will be equal to the area under the stress-time curve. If the thickness of B is less than half the wavelength, the momentum trapped in it is equal to:-

$$M = \int_0^T \sigma(t) dt$$

where $\sigma(t)$ = stress at time t

T = time for wave to travel twice the thickness of B.

By varying the thickness of B and measuring its momentum, a stress-time curve can be constructed.

The mechanism of scabbing is clearly very similar to this. If we consider a compressional wave with an instantaneous rise time and a gradual decay, produced by detonating explosive, transmitted into a steel plate, it will be reflected from the free surface as a tension wave, as described above and shown in fig. 2. The unbroken line represents the resultant stress pattern after reflection. Clearly, with increasing time the resultant tensile

stress (ab) moves further into the plate and increases in amplitude. When the amplitude (ab) becomes equal to the dynamic tensile strength of the material, Y_D , fracture occurs. It is important to note that fracture occurs at a distance from the surface, δ , equal to one half the distance within the stress wave corresponding to a fall in stress equal to the tensile strength. Hence scab thickness is a direct indication of the rate of decrease of stress behind the wave front and is independent of the height of the front, provided that the stress is large enough to cause scabbing.

Rinehart (6) has reported a series of experiments in which he used a Hopkinson technique to study the shape of the stress pulse applied to steel plates by cylinders of explosive. He used cylinders of explosive 1 in. diameter and 2 ins. long, placed on steel plates 1.5 to 3 ins. thick. Small pellets of steel 1/16 to 3/4 in. thick were stuck to the free face on the axis of the charge and their velocities measured. With this data, and assuming a constant wave velocity equal to the elastic wave velocity (V_e), a stress-time curve was calculated (fig. 3) from the equation

$$\sigma = \rho V_e v$$

where ρ = density
 v = velocity

It should be remembered that all the plates used were too thick to allow the scab to detach and that in many cases the wave amplitude is only slightly greater than the yield stress. It will be seen below that it would probably be better to use a velocity rather lower than the elastic velocity. Fig. 3 shows clearly that the amplitude of the wave-front decreases rapidly with plate thickness, but that the later stress increments tend to become larger. Rinehart suggests that energy may be fed from the front of the wave to the back if different parts of the wave are transmitted with different velocities. It was found that a 1.5 in. steel plate gave a scab 0.14 ins. thick and that 2 and 2.5 in. plates gave cracks 0.17 and 0.25 ins. from the surface, while 3 in. plates showed no cracks. Using this data, attempts were made to calculate the critical fracture stress; the results were rather varied but were between 1 and 1.5×10^{10} dynes/cm².

In another paper (7) Rinehart has studied the dimensions of the crater produced at the explosive-metal interface and also the metallurgical properties of the attacked steel. Charges 2 ins. long were fired against steel plates. It was found that immediately beneath the crater, which was approximately conical in shape, there was a region of very severe cold-working, the volume of which increased as the volume of the crater. Some dimensions are shown in Table I below.

Table I

Dis. of charge (ins.)	Depth of crater (ins.)	Total cone angle (deg.)	Thickness of cold-worked region (ins.)	Volume of Crater (in. ³)	Volume of cold-worked region (in. ³)
0.5	0.059	152	0.157	0.002	0.032
1.0	0.138	156	0.258	0.073	0.231
1.5	0.216	159	0.334	0.162	0.784
2.0	0.276	161	0.394	0.51	0.67

The shape of the crater may throw some light on the stress distribution across the explosive-metal interface, although the precise quantitative relation is not known. The depth of the crater is most likely to be determined by the total impulse, although the shape of the stress-time curve is probably important.

Rockwell hardness measurements were made on sectioned samples and lines of equal hardness were plotted. A typical example is shown in fig. 4. The highly worked region beneath was much harder than the rest of the material. Photomicrographs of the various regions were also shown; the region beneath the highly worked region contained many shock twins.

Hill (20) has reported the results of a large number of static firings against armour plate; he studied charges 2-5 ins. long and armour 4, 6 and 8 ins. thick. The following conclusions were reached:-

- (1) For a scab to be formed a critical area of explosive-metal interface must be exceeded for a given plate thickness.
- (2) The scab weight is independent of charge shape and the thickness and hardness of the armour.
- (3) The scab weight in lbs. = $0.046 (\text{charge area, in}^2)^{1.5}$.
- (4) Scab area = $1.5 \times \text{charge contact area}$.
- (5) Scab thickness = $0.096 \times \text{charge contact diameter}$.
- (6) Critical armour thickness for no scabbing = $1.4 (\text{charge contact diameter})^{0.75}$.

This work covered a fairly large range of charge parameters and the above expressions are no doubt approximately true, but the scatter of points on the graphs is very considerable in some cases. Our results do not altogether agree with these empirical equations, although it must be remembered that the results are for armour plate, whereas our experiments are with mild steel.

FVIE (8) have done some static tests of cylindrical charges of plastic explosive against armour plate. They found the ratio of critical plate thickness to charge contact diameter for scabbing to occur was 1.06 for plates 0.5 in. to 1.75 ins. thick. Hill's experiments showed that this factor increased to about 1.25 for 8 in. plates. FVIE described the general appearance of all the scabs. The depths of the craters formed by the explosive agreed quite closely with Rinehart's results reproduced above which were for mild steel.

Before discussing the work on the mechanism of the scabbing process, it will be useful to mention briefly the various waves that can be propagated through materials. When a wire or relatively thin rod is subjected to an impact of relatively small magnitude, so that the elastic limit of the material is not exceeded, a longitudinal wave is propagated along it with velocity:

$$v = \left(\frac{E}{\rho} \right)^{\frac{1}{2}}$$

where E = Young's Modulus
 ρ = density of the material

In an extended solid, however, lateral strains are prevented so that lateral stresses are set up and it can be shown that the propagation velocity is given by an equation containing any two of the constants, Young's Modulus, bulk modulus, rigidity modulus, and Poisson's ratio. A convenient equation is

$$v_s = \left(\frac{K}{\rho} \cdot \frac{1-\nu}{1+\nu} \right)^{\frac{1}{2}}$$

where K = bulk modulus
 ν = Poisson's ratio

Using the following data for mild steel

$$\begin{aligned} K &= 16.7 \times 10^{11} \\ \rho &= 7.83 \text{ g./cm.}^3 \\ \nu &= 0.289 \end{aligned}$$

it is found that $V_0 = 5950$ m./sec. A value very close to this has been obtained by Pack, Evans and James (9) under conditions very similar to those used in the present work. Hughes et al (10) have quoted 5880 m./sec. and Pay and Vortier (11) 5950 m./sec.

When the yield value of the material is exceeded, as in solids at higher stresses or in liquids at all stresses, the propagation velocity (V_p) is determined only by the density and bulk modulus by the equation

$$V_p = \left(\frac{K}{\rho}\right)^{\frac{1}{2}}$$

Using the same data as above for mild steel, V_p is found to be 4620 m./sec; it should, however, be noted that this value will only be found for relatively low stresses, since at higher stresses K and ρ will both take on different values.

It is only possible to obtain a complete picture of the wave propagation in a solid if a complete stress-strain diagram of the material is available; this must also represent the relationship at the appropriate rate of strain and not under the usual static conditions. Such complete information for the type of problem under consideration is never available. The stresses involved in a detonation wave are of the order of 2×10^{11} dynes/cm.². Bridgman's (12, 13) data on compressibility go up to about 2×10^{10} dynes/cm.² so that drastic extrapolations are necessary, and, in any case, it has been shown that both compressibility and yield value are functions of rate of strain. No experimental technique other than the use of explosives can apply these pressures sufficiently rapidly, i.e. in times of less than 10^{-7} secs. Bridgman's data on the compressibility of steel up to 2×10^{10} dynes/cm.² are represented by an equation of the type:-

$$-\frac{\Delta V}{V_0} = Ap - Bp^2$$

where

$$\begin{aligned} \Delta V &= \text{Volume change} \\ V_0 &= \text{Initial volume} \\ p &= \text{Applied pressure} \\ A &= 5.94 \times 10^{-13} \\ B &= 0.6 \times 10^{-24} \end{aligned}$$

Pack, Evans and James (9) used an equation developed on theoretical grounds assuming that the pressure increases exponentially with interatomic distance

$$p = \alpha \left[\exp \beta \left(1 - \frac{\rho_0}{\rho}\right) - 1 \right] / \left(\frac{\rho_0}{\rho}\right)^{2/3}$$

in which α and β are calculated from Bridgman's empirical data at lower pressures. The values used were $\alpha = 120.16 \times 10^{10}$ dynes/cm.² and $\beta = 4.203$ for mild steel. The pressure-density data obtained from these two equations are shown in Table II below.

Table II

p (dynes/cm. ²)	Bulk modulus (dynes/cm. ²)		Density (g./cm. ³)	
	Bridgman	Pack	Bridgman	Pack
0	1.67×10^{12}	1.67×10^{12}	7.83	7.83
1.1×10^{11}	1.90 "	1.86 "	8.30	8.31
2.0 "	2.11 "	2.02 "	8.64	8.68
3.0 "	2.41 "	2.17 "	8.92	9.07

The type of wave associated with the propagation of a finite stress into a metal has been studied extensively by von Karman (14) and others for fairly high rates of strain but much lower than those associated with explosives. The form of the wave was deduced from the static stress-strain curve and was shown to consist of two parts; firstly a wave of elastic deformation of magnitude equal to the dynamic yield stress of the material is propagated with the velocity V_0 discussed above, and secondly a wave of plastic deformation propagated with a lower velocity calculated from the slope of the stress-strain curve at the particular stress. It seems certain that the wave of plastic deformation develops into a shock wave with a steep front since Table II above shows that the bulk modulus increases with pressure, so that higher stresses are propagated with ever-increasing velocity. Quite clearly, interatomic forces will reduce compressibility at the very high stresses associated with detonation waves.

The shock wave velocity and associated particle velocity can be calculated from the equations of continuity and momentum according to the original method of Rankine and Hugoniot

$$\rho(U-u) = \rho_0 U \text{ (continuity)}$$

$$p = \rho_0 Uu \text{ (momentum)}$$

where ρ_0 = initial density
 ρ = final density
 U = shock wave velocity
 u = particle velocity
 p = pressure jump at shock front

Since p can be obtained as a function of ρ from the above equations, U can be obtained as a function of p . The relationship is shown in Table III below and in fig. 5.

Table III

p (dynes/cm. ²)	U (m./sec.)
5×10^{11}	4650
10 "	4800
15 "	4930
20 "	5050
25 "	5160
30 "	5260

Since our knowledge of the dynamic stress-strain relationship is so scanty, it is difficult to predict the shape of the stress-displacement curve between the two discontinuities. It is assumed that the curve is of the form shown in fig. 6. The static yield stress can be taken to be about 7.7×10^9 dynes/cm.² and there is some evidence (6) that the dynamic yield stress (Y_D) is rather higher and possibly about 10^{10} dynes/cm.².

It has been pointed out above that the shape of the stress-time curve in the steel is of primary importance in determining the characteristics of the scab formed. The shape is determined by two factors: firstly the shape of the pressure-time curve in the detonation zone, and secondly the way in which this is modified by the steel. The information on the shape of the pressure-time curve is rather scanty. It can be assumed that the rise to the peak pressure is essentially instantaneous and the usually accepted figures are for TNT 1.49×10^{11} and for plastic explosive 1.63×10^{11} dynes/cm.² (15).

Hill and Pack (16) have investigated the problem of the expansion of gases behind a detonating slab of explosive. They considered the two-dimensional case of a slab of T.M.T. of infinite length and breadth but 2.0 cms. wide and obtained values for the pressure as a function of distance behind the detonation front at various distances from the axis of symmetry. In particular, they found that the pressure had fallen to about one-tenth of its initial value in a distance behind the detonation front equal to the charge width, so that charges of lengths greater than this can be regarded as effectively infinite; their results are shown graphically in fig. 7, in which the figures on the curves indicate the distance in cms. from the charge axis in each case. The difference between this case and that of an infinite cylinder of explosive, to which our charges usually approximate, lies in the introduction of a third dimension. However, the problem is then symmetrical in the plane at right angles to the charge axis, and we should expect the shape of the pressure-distance curves to be much the same as those of the two-dimensional case. The main difference must be that the pressure falls off more rapidly with distance from the axis. At least we have a qualitative picture of the variation with time of the pressure at the explosive-steel interface; we expect the stress propagated into the steel to be of the same form but modified in magnitude by the boundary conditions.

If we knew the exact stress-time relationship of the pulse incident on the metal surface, we could, in fact, solve the problem of the propagation of the stress through the steel, assuming the case to be one-dimensional and provided that we had also a complete knowledge of the dynamic stress-strain curve and neglected all attenuation effects. Chorlton (17) has carried out an analysis of this nature for the plane-wave case. In this analysis Chorlton used the method of characteristics due to Bohnenblust (18) and determined the stress-time pattern in a laterally infinite plate subject on one face to a stress pulse of two different hypothetical types; the first was a finite pulse of constant stress and instantaneous decay, and the second a finite pulse of constant stress which decayed exponentially. He also assumed an idealised stress-strain curve of the type shown in fig. 3 and postulated various types of attenuation of the plastic wave which seem physically unlikely. In view of the assumptions made it is not surprising that the results obtained are in poor agreement with experiment. Even if the assumptions necessary could be allowed, the problem when extended to more than one dimension becomes mathematically intractable.

After interaction with the steel surface it has been shown (9) that the initial pressure in the steel is about 2.83×10^{11} dynes/cm.². The best assumption that can be made at present is that the shape of the stress-time curve is qualitatively similar to that obtained for TNT by Hill and Pack (16). Clearly, in the case of the three-dimensional problem, it will be extremely difficult to solve quantitatively the problem of the shape of the stress-time curve after travelling a given distance into the steel.

It seems that the shape will be modified by three effects:-

- (a) lateral expansion of the wave in the steel
- (b) attenuation by unloading waves from behind
- (c) reduction in amplitude due to work done.

In dealing with the propagation of unloading waves it is usually assumed, e.g. Chorlton (19), that they behave as elastic waves and so tend to overtake the shock wave associated with plastic deformation. It can be seen from fig. 8 that, since permanent deformation is involved, an unloading wave must travel faster than the shock-front, although it may not reach the elastic wave velocity and may not have the same velocity for all values of the stress. As the elastic wave catches up the shock wave attenuation must take place.

3. Experimental Methods

The experimental objective was to determine how the following quantities vary with charge dimensions and plate thickness when cylindrical charges of plastic explosive are fired against steel plates:-

- (1) The velocity of the plastic wave (in this case a shock-wave) through the steel.
- (2) The velocity of the back surface of the plate and its variation with distance over distances up to approximately 0.5 in.
- (3) The shape and dimensions of the scab formed and other damage to the plate.

3.1 Recording Technique

The essential requirement in this type of work is an instrument capable of measuring extremely short-time intervals over a period of about 40 microseconds to within 0.01 microseconds. Even the best of the conventional linear sweep oscillographs give traces which are not capable of such high resolution. The spiral-trace oscillograph, recently developed in A.R.E., has been found to be particularly suited to the exacting requirements of this work and has been used throughout. In this oscillograph two sine-waves of identical frequency, but 90° out of phase, are applied simultaneously to the X and Y plates. The amplitude of the oscillation is steadily decreased, at the same time as the beam brightening pulse is applied, thus producing a spiral trace starting from the edge of the tube and moving inwards. In the particular instrument used, the time per revolution was 2 microseconds and the number of revolutions about 20. The centre of the spiral does not lend itself to easy measurement, but there is no difficulty in measuring up to 30 microseconds to ± 0.01 microseconds. In our experiments the measurement of time intervals did not become a limiting factor. A second advantage of the spiral trace is the greater ease with which records can be measured compared with a linear one; by projecting an image of the trace on to a circular scale graduated in 200 divisions each representing 0.01 microseconds, any interval on it can be read off directly. The specially designed single shot camera employed for recording traces incorporated a Wray 2 in. f/1.0 lens and used standard 35 mm. film. Ilford 50 91 film developed for 5 minutes at 20°C. in I.D. 33 gave satisfactory results.

As in other methods of electronic time recording, the particular events to be recorded must be converted into electronic pulses, which are then suitably injected into the recording instrument. The pulses were obtained by using as events the closing of electrical circuits containing resistance and capacity. The type of circuit used is shown diagrammatically in fig. 9. Values of $C = 300$ pf and $R_2 = 100$ ohms

gave pulses of suitable duration. R_1 is a high resistance (1 megohm) and the D.C. voltage is suitably \pm 300 volts, its sign determining the sign of the pulse developed. C is charged through R_1 by the 300 volts supply and thereafter no current flows. On closing the gap (S) one plate of C is earthed and a high frequency pulse is developed in the $R_2 - C$ circuit. The pulse is transmitted to the recording instrument by a coaxial cable (A). It is necessary to terminate A at the oscillograph by a 100 ohm resistance to earth, to prevent pulse reflection in the cable.

The pulses produced in this way are injected into either the grid or cathode of the cathode-ray tube and appear on the trace as short lengths of beam-brightening or suppression, according to their original sign and their point of application to the oscillograph. It is convenient to produce a sequence of events alternately positive and negative so as to have a means of partially identifying oscillograph events with actual events.

The oscillograph is triggered by a larger positive pulse ($R_2 = 100$ ohms, $C = 0.03 \mu F$), about 2 microseconds prior to the first event. This simultaneously triggers the sweep and produces beam brightening. The overall delay in triggering is about 0.2 microseconds. A typical trace is shown in Plate I.

3.2 The Charges

The charges consisted of rolled paper cylinders filled with plastic explosive by hand-stemming; no. 8 Briks detonators were inserted about $\frac{1}{2}$ in. into the end of the charge and held in place symmetrically by means of a well-made wood block. The charges were fired horizontally and were held in contact with one of the machined surfaces of the steel plates either by supporting on V-blocks or by means of Durafix.

The steel plates used were of mild steel and had properties shown in Table IV below.

Table IV

Spectrographic Analysis

Element	Plate	Bar
C	0.12%	0.14%
Si	0.04	0.07
Mn	0.48	0.64
Ni	0.05	0.19
Cr	0.04	0.05
Mo	0.01	0.01

Diamond Pyramid Hardness

Load	Plate	Bar
30 Kg.	127	126

It was found that the variation in properties did not appreciably affect the results obtained. The plates were all square and machined to give surfaces flat to better than 0.001 ins. The dimensions of the plates were varied with the diameter of the charge to maintain an

effectively infinite plate, as shown in Table V below.

Table V

Charge Diameter (ins.)	Plate Dimensions (ins.)
1	4
2	6
3	12

The combinations of charge dimensions and plate thicknesses are shown in Table VI.

Table VI

Charge Length (ins.)	Charge Diameter (ins.)		
	1	2	3
1	1 in.		1 in. 2 ins.
1.5	1 in.	1 in. 2 ins.	
2	1 in.	0.2 in. 0.3 in. 1 in. 2 ins.	1 in. 2 ins. 3 ins.
3	1 in.	1 in. 2 ins.	
4	1 in.	1 in. 2 ins.	1 in. 2 ins.
8			2 ins. 3 ins.

3.3 The Event Systems

Three types of event were required:-

(1) The Trigger Event

This consisted of a G.B. head, which is essentially a pair of insulated copper wires twisted together and mounted in plastic so that the bare ends of the wire are close together and flush with the plastic surface without actually being in electrical contact. As the detonation wave, which contains ionized gases, passes the detector, the wires are effectively short-circuited and thus produce a pulse to trigger the oscillograph. The detector was inserted into the charge through a hole in the paper tube at a distance from the steel plate to give the correct delay.

(ii) The Wire Event

The arrival of the detonation wave at the surface of the plate was detected by placing a length of enameled wire between the explosive and the plate. On arrival of the detonation wave at

the plate the wire was short-circuited to the plate which was earthed. The event occasionally occurred prematurely or was missed altogether; this was attributed to gas jets between the explosive and the paper tube. The difficulty was eliminated by covering the wire near the edges of the charge with plasticene.

(iii) The Probe Events

The movement of the face of the steel plate was followed by means of wire probes situated at various distances from the plate. Two sets of distances were generally used as follows:-

(a) 2, 5, 10, 15, 20 and 25 thousandths of an inch.

(b) 2, 25, 50, 100, 150 and 200 thousandths of an inch.

The probes consisted of short lengths of about 0.5 in. of 22-gauge copper wire soldered into holes drilled axially into 6 BA brass screws. The screws were mounted on Tufnol sheets in holes tapped at an angle of about 70° to the surface, so that the ends of the wires formed a small circle about 0.3 in. in diameter around the axis of the charge. The distances of the probes from the plate were accurately adjusted by means of feeler gauges and they were then secured in position by means of lock nuts. Each probe formed part of an event circuit, the steel plate acting as a common earth, so that as the steel plate touched each probe a pulse was produced on the oscillograph. The system is shown diagrammatically in fig. 10 and a typical charge is shown in Plate II.

With the 3 in. charges more information was obtained by using three rings of probes instead of one, to investigate the various velocities as a function of distance from charge axis. In this case the probes were all normal to the surface of the Tufnol plate and the rings had radii of 0.25, 0.75 and 1.25 ins. Each ring was connected to a separate oscillograph. The wire event was replaced by three separate wires, one along a diameter of the charge and the other two parallel to the first but, respectively, 0.75 and 1.25 ins. from it. The trigger event was used to trigger all three oscillographs. Complications arose with the normal circuits because the common earth system and close proximity of leads caused all the pulses to appear on all the oscillographs. Each set of events had a separate event box, each being isolated from the others and the earth points in each being connected to the real earth point through a high resistance. All the boxes had a symmetrical construction. A separate earth to the plate was used with each set of events and all the leads of one set were twisted together. The three wire events were applied to the grids of the tubes of all three oscillographs to allow time synchronization. The pulses from each ring of probes were applied to the cathode of each tube. Probe distances of 2, 10, 25, 50, 200 and 400 thousandths of an inch were used with these charges. A typical charge is shown in Plate III.

4. Experimental Results

It seems of little value to tabulate the measurements made concerning the surface displacement of the steel plate. These results are shown graphically in figs. 11 to 14. The derivation from these results of both the velocity and amplitude of the shock-wave requires discussion, and the values obtained are given during the discussion in Table IX.

The following observations may be made on the displacement-time graphs. The complications introduced by the fracture process make it impossible to

attach fundamental significance to the velocity of the surface over the whole distance, while the significance of the initial part of the curve is discussed below. The general features of the curves, however, can be summarized. The curves taken near the axis of the charge over the first 200×10^{-3} in. never show a marked discontinuity at any point, although, if we consider those plotted over the first 25×10^{-3} in., then a discontinuity is detected in several cases. The curves are either linear or show a slight deceleration over the region 25 to 200×10^{-3} in., the latter alternative being most apparent when the charge length is small. For a given charge diameter, the slopes of the curves become greater with decreasing plate thickness and increasing length; but in the latter case they tend to a maximum value, equal to the initial slope, so that the effect of length is small after the ratio of charge length to diameter becomes approximately two. In general, the slopes do not scale; for example, a 1 in. long by 1 in. diameter charge against a 1 in. plate results in a much smaller velocity than does a 2 in. long by 2 in. diameter charge against a 2 in. plate.

In our experiments involving three concentric rings of probes, we were able to obtain some data concerning the variation of surface velocity with radial distance from the centre of the plates. The three distances chosen were 0.25, 0.75 and 1.25 in., and in describing the results it will be convenient to call the sets of points, corresponding to these distances, A, B and C, respectively. The results are shown graphically in figs. 15 to 17.

Only one result was obtained for a 1 in. plate, and that with a charge 2 in. long. The displacement-time curves show that the points A and C move with the same linear velocity over the first 0.2 in. After this the velocity of A remains constant up to 0.4 in., but the velocity of C decreases slightly. A difference in velocity of one point on the surface relative to another indicates a change in the curvature of the plate surface with time. This effect is independent of the slight surface curvature produced by the non-planarity of the shock-wave; curvature of this type is shown by the displacement of the curves along the time axis. The measurements accord with the fact that the final scab is almost flat over the region of the probes.

The curves for the 2 in. plates indicate that for each charge length the velocities of A, B and C are constant and equal over at least the first 0.05 in., although their magnitudes depend on the charge length. Hence the plate surface, over the area of measurement, moves through 0.05 in. without change of curvature. Subsequently the velocities decrease, the change being greatest for points C. The results for the 4 in. long charge (fig. 16c) show that the surface becomes increasingly curved over the distances 0.05 to 0.4 in. On the other hand, the difference in velocity between points A and C, for an 8 in. long charge (fig. 22d), is only small, so that the rate of increase of curvature is also comparatively small.

The velocities of points A, B and C in the case of the 3 in. plates are, for each length, linear and equal over the first 0.025 in. As before, the velocities then decrease, although for both the 2 in. and 8 in. long charges the decrease for points A is quite small. Points C, however, undergo an appreciable drop in velocity, followed by an increase, so that after 0.06 in. their velocity is again about equal to that of A. The effect is observed in both cases (figs. 17a and 17b).

In presenting the measurements made on the damage to the plate, we have tabulated in Table VII the following dimensions:- the diameter of the hole left by the scab, the thickness of the scab at the edge, the thickness of the scab at the centre, and the depth of the crater formed at the explosive-steel interface, for each combination of charge and plate. The first three quantities have been expressed as the mean value of several measurements, and where more than one example of any particular charge-plate combination has been obtained, the values given are a mean for those examples. The error associated with the scab thickness measurements are in all cases ± 0.05 cm. and in the crater depth about ± 0.02 cm., while the scab diameter is liable to an error of ± 0.1 cm.

Table VII

Plate Thickness (ins.)	Charge Diameter (ins.)	Charge Length (ins.)	Depth of Crater (cms.)	Diameter of Scab Hole (cms.)	Thickness of Scab at Edge (cms.)	Thickness of Scab at Centre (cms.)
1	1	1	0.26	-	0.22	0.27
		1.5	0.40	4.2	0.26	0.36
		2	0.43	4.2	0.27	0.38
		3	0.48	4.5	0.30	0.40
	2	4	0.41	4.1	0.25	0.35
		1.5	0.94	7.2	0.25	0.60
		2	1.04	7.0	0.25	1.04
		3	1.10	7.0	0.26	0.90
		4	1.11	7.0	-	1.08
	3	1	-	10.9	0.30	-
		2	-	10.6	0.26	-
		4	-	10.7	0.28	-
2	2	1.5	0.64	8.0	0.52	0.65
		2	0.67	7.3	0.52	0.62
		3	0.82	7.8	0.53	0.47
		4	0.92	7.8	0.54	0.45
	3	1	0.66	11.3	0.48	1.2
		2	1.00	13.0	0.56	1.2
		4	1.55	11.9	0.51	1.5
		8	1.58	12.5	0.74	1.7
	3	2	1.07	13.1	0.68	0.90
		8	1.50	11.5	0.80	0.80

For each case we have shown diagrammatically in figs. 18 to 23 a cross-section through the plate taken along a charge diameter, in order to illustrate the main features of the damage pattern obtained in the steel. It will be convenient here to summarize these features.

(1) The Crater

The depth of the crater at any point may be considered as a measure of the total impulse applied to the plate at that point. A consideration of Table VII shows that the crater depth, which has in all cases been measured on the charge axis, tends, for a given charge diameter, to a limiting value, which is reached when the charge length to diameter ratio becomes appreciably greater than unity. We see also that this limiting value is approximately proportional to the charge diameter and that it is little affected by the plate thickness provided this is not very small compared with the charge diameter. Most of the craters are conical in shape. The only case in which a direct comparison can be made with Kinsch's results, quoted in Table I, shows good agreement.

(2) Diameter of Scab Hole

If the plate thickness to charge diameter ratio is maintained, then the scab diameter is roughly proportional to the charge diameter, the factor of proportionality being about 1.5. The diameter decreases somewhat with decreasing plate thickness for a given charge diameter but appears in all cases to be independent of charge length. The variation of the ratio of the diameter of the scab hole to the diameter of the charge is believed to be due to two causes: firstly, the

lateral expansion of the shock-wave in the steel and, secondly, the extension of the primary scabbing fracture due to the momentum of the scab after this fracture.

(3) The Scab Thickness

This quantity is of particular interest as it can give an indication of the shape of the stress-wave propagated through the plate. It is noticeable that the thickness at the edge is approximately constant for a given plate thickness, regardless of the charge used, and that it is roughly proportional to the plate thickness. Further, provided the charge diameter does not exceed the plate thickness, the scab thickness is roughly uniform over the scab area. On the other hand, when the charge diameter is greater than the plate thickness, the scab is by no means of uniform thickness and is much thicker at the centre. The thickness at the centre is dependent on both charge length and diameter and there is some indication that it reaches a maximum value at constant diameter when the ratio of charge length to diameter becomes greater than unity.

In addition to the main scabbing surface, other fracture surfaces are often developed in the plate. In particular it was noticed in the 3 in. plates that fractures parallel to the main scabbing surface are evident and are particularly well developed with the longer charge.

In general the fracture surfaces are coarsely crystalline in appearance for the material cut from bar. In the few cases where the steel was cut from 1 in. plate, the fracture surfaces are not crystalline in appearance and seem to follow definite planes in the material. The edges of the scabs are of the same appearance as the scabbing surface, suggesting that they are the result of tensile breaks; this may be compared with the edges of scabs obtained from armour plate, which are typical, in appearance, of shearing fractures. In a few cases a well defined surface of finely crystalline appearance occurs in the centre of the scabbing surface area. This is so only for the larger charges, and it is possible that the fracture here occurs in a severely 'cold worked' region.

5. Discussion of Results

It has been shown above that when a piece of mild steel is subjected to a transient stress wave the amplitude of which is much greater than the dynamic yield stress (Y_p), two discontinuities are propagated into the steel. The first of these has an amplitude equal to the dynamic yield stress and its velocity is equal to the elastic wave velocity (V_e). This is followed by a second wave which is steep fronted, of amplitude which continually diminishes with distance travelled, and has a velocity which is less than V_e and is a function of the amplitude.

It is now necessary to consider what happens when a stress wave of this kind reaches a free surface, as in our experiments. For a plane discontinuity of finite compressive stress approaching a free surface normally, the condition of zero pressure at the surface requires that the compressive stress should be reflected normally as a tension of equal magnitude and thus result in a doubling of the particle velocity in the region through which the tension has travelled. Provided that the compressive stress is maintained in amplitude, the surface will move out with a constant velocity equal to twice the particle velocity associated with the same stress wave before reflection (19). Applying the argument to our particular case in which a discontinuity of maintained amplitude equal to Y_p is followed by a second discontinuity of much greater amplitude p , which it is assumed is maintained, it is seen that the surface will first move with a velocity determined by Y_p and subsequently change its velocity abruptly to one determined by p .

This is shown graphically in fig. 2A, in which surface displacement is plotted against time; the displacement zero is taken as the initial position of the surface and the time zero is arbitrary.

The time interval $t_g - t_s$ represents the time between the arrival of the two discontinuities at the surface and depends upon the distance travelled through the plate. The slopes V_{FE} and V_{FS} , representing the surface velocity due to reflection of the elastic wave and shock wave respectively, are given by

$$V_{FE} = 2 u_g$$

$$V_{FS} = 2 u_s$$

where u_g and u_s are the particle velocities associated with the elastic wave and the shock wave. It has been seen that, in general across a discontinuity,

$$p = \rho_0 U$$

so that we may write

$$V_{FE} = \frac{2 Y_D}{\rho_0 V_E}$$

$$V_{FS} = \frac{2 p}{\rho_0 U}$$

where in the second equation we have neglected any effect due to the elastic wave.

It will now be convenient to take an explicit example. Let a single plane discontinuity of finite compressive and maintained stress p (where $p \gg Y_D$) be initiated at time $t = 0$, at a distance d from a free surface so that it propagates normally towards it. The discontinuity will be divided into two parts, being the elastic and shock waves, as we have seen. Using the following data, in which the choice of U and p is dictated by experimental results

$$\begin{aligned} V_E &= 6000 \text{ m./sec.} \\ Y_D &= 10^{10} \text{ dynes/cm.}^2 \\ U &= 5000 \text{ m./sec.} \\ p &= 10^{11} \text{ dynes/cm.}^2 \\ \rho_0 &= 7.83 \text{ g./cm.}^3 \\ d &= 5.00 \text{ cms.} \end{aligned}$$

it is found that:-

$$\begin{aligned} t_g &= 8.33 \text{ microseconds} \\ t_s &= 10.00 \text{ microseconds} \\ V_{FE} &= 42.5 \text{ m./sec.} \\ V_{FS} &= 512 \text{ m./sec.} \end{aligned}$$

The displacement of the surface at time t_g is thus $S = 6.4 \times 10^{-3}$ cms., and in general S is directly proportional to d . We have throughout neglected the effect of the elastic wave on the shock wave and consider any error so introduced to be negligible. It follows from these considerations that given d and knowing the whole displacement-time curve relative to $t = 0$, we may calculate V_E , U , Y_D and p . On the other hand, if we have points only over the range determined by the shock wave, then we cannot directly determine the value U from our graph. We may, however, from

assumed values of V_E and I_D , construct the 'elastic part' of the graph and thence by extrapolation of the 'shock wave part' we can calculate U . Furthermore, even though the values of V_E and I_D may be somewhat uncertain, the error introduced into the time co-ordinate of the intersection of the two parts of the curve (t_E) is considerably smaller. We have taken as an example the values

$$\begin{aligned} V_E &= 6000 \text{ m./sec;} & \Delta V_E &= \pm 100 \text{ m./sec.} \\ I_D &= 10^{10} \text{ dynes/cm.}^2; & \Delta I_D &= \pm 0.4 \times 10^{10} \text{ dynes/cm.}^2 \\ \text{therefore } V_{FE} &= 42.5 \text{ m./sec;} & \Delta V_{FE} &= \pm 18 \text{ m./sec.} \end{aligned}$$

and thence have shown graphically that

$$\Delta t_E = \pm 0.06 \mu\text{S.}$$

In general, it follows that U will not be in error by more than 0.6% from this cause.

The system so far dealt with is an idealised one. In our experiments we have detonated a charge of explosive of finite dimensions against a steel plate also of finite dimensions. We have recorded what we consider to be the arrival of the detonation wave at the plate surface, in the centre of the charge, and referred to this zero of time we have recorded the arrival of the further plate surface at points of predetermined distance from its initial position and somewhat displaced from the charge axis. We do not doubt that the lateral dimensions of the plates in all our experiments are effectively infinite. The length of the charge introduces a non-planarity into the detonation wave and therefore also into the stress wave through the plate. As a result the surface of the plate moves first on the axis of the charge and subsequently at distances from this axis. We correct for this effect by determining graphically the difference between the times of arrival of the shock wave at the surface, on the axis and at distances 3 mas. and 6 mas. from it. These distances correspond to the radial displacements at which we measured the surface velocity in two sets of experiments. The calculation is made for each charge and plate combination, assuming values of the detonation velocity $V_D = 7800 \text{ m./sec.}$ and shock-wave $U = 5000 \text{ m./sec.}$, and using Huygen's construction for the wave propagations. The time difference is then subtracted from our experimentally determined time of arrival of the shock wave at the plate surface, to give the true time of traverse through the plate. The correction is small and in most cases less than 0.03 micro-seconds. We believe that any non-planarity of the wave will not sufficiently affect the elastic wave velocity to introduce any appreciable error into our method of shock-wave velocity calculation.

The good agreement found between the theoretical and experimental times of arrival of the detonation wave at distances displaced from the charge axis is good evidence that the time zero is recorded correctly. Table VIII shows the times of arrival of the detonation wave at distances, d , from the axis of a cylinder of explosive 2 ins. long and 3 ins. diameter, detonated centrally at one end.

Table VIII

d (ins.)	Time (experimental) (μS)	Time (theoretical) (μS)
0	0	0
0.75	0.43	0.44
1.25	1.19	1.17

We conclude that any error in the time zero is due to the recording technique and is about ± 0.01 microseconds.

Our method of shock wave velocity determination depends upon an extrapolation of the surface displacement, due to shock-wave reflection, back to the time t_0 corresponding to a displacement in the two-inch plate case of about 6.4×10^{-3} cm. Even in those cases where we have measured the displacement time at 5×10^{-3} in. intervals, in order to make the extrapolation we must be able to assume that the curve is approximately linear over the first three or four points, if we are to obtain reasonable accuracy in our result. This is particularly true in view of the substantial error associated with the displacement measurement. In general the inaccuracy in the location of the probes used must be at least $\pm 0.5 \times 10^{-3}$ in., and using this value we have estimated graphically that the error in determining a time co-ordinate by linear extrapolation is about 0.03 microseconds.

In order to determine how far the curve is likely to be linear, that is, how long the maximum stress in the shock wave will be maintained, we must consider the phenomenon of scabbing. This has been discussed above. The point of importance is that in the time taken for the shock-wave to travel twice the thickness of the scab, the pressure must have fallen by an amount equal to the tensile strength of the material; the statement neglects attenuation of the shock front at the surface but remains approximately true. For plates 2 ins. thick we have never observed a value of scab thickness less than 0.40 cm., and using this value we find that the time taken to fall by about 10^{10} dynes/cm.², which is an approximate value of the dynamic tensile strength given by Rinehart (6), is about 0.7 microseconds. Assuming a stress at the wave front of 10^{11} dynes/cm.², we conclude that in this case the stress falls from 10^{11} to 0.9×10^{11} dynes/cm.² in 0.7 microseconds, the corresponding face velocities being 500 and 450 m./sec. respectively. In this time the surface will have been displaced by 12×10^{-3} in. We may expect then that the displacement curve will be approximately linear over at least this distance, and a linear extrapolation over this distance is justified. Subsequent behaviour is complicated by the fracture process, and we are unable to derive the expected surface behaviour at later times. The considerations given, however, justify our extrapolating from measurements made at 5×10^{-3} in. intervals over the first 25×10^{-3} in. On the other hand, if our first measurement is made at 25×10^{-3} in., we have no justification for extrapolation unless we have determined empirically the shape of the curve over the first 25×10^{-3} in; even then our extrapolation is liable to considerable error.

In addition to the experimental errors already discussed, we have an uncertainty in the absolute value of the displacement. The probes themselves are placed at intervals which we have stated as subject to an error of $\pm 0.5 \times 10^{-3}$ in., but owing to the method of support, there is a probability that the whole probe system may be moved relative to the plate surface after setting up the experiment. This is likely to introduce an error of $\pm 1 \times 10^{-3}$ in. in the absolute displacement value, with a resultant error of ± 0.05 microseconds in the time determination.

From our experimental results we have selected those cases for which we deem justified a linear extrapolation of the displacement curves, and for these cases we have made the corrections indicated and determined shock wave velocities by the method described. We consider that our overall experimental error will be about ± 0.08 microseconds, corresponding to an error of ± 80 m./sec., ± 40 m./sec. and ± 30 m./sec., for determinations over 1 in., 2 ins. and 3 ins. respectively. The values we obtain are shown in Table IX. Of these values the nine starred ones were obtained from curves measured over 5×10^{-3} in. intervals and are the most reliable. The initial face velocities over the linear part and the corresponding stresses as calculated from the equation

$$2p = \rho_0 V_{FS} U$$

using the theoretical values of U obtained from our plotted $U(p)$ curve, are also given in the table. The errors associated with these values are of the order $\pm 5\%$. The charge and plate combinations with which our values are associated are shown with approximate dimensions only.

Table IX

Charge Length (ins.)	Charge Diameter (ins.)	Plate Thickness (ins.)	U (m./sec.)	V_{FS} (m./sec.)	P (dynes/cm. ² $\times 10^{10}$)
8	3	3	4980 X	425	7.9
2	3	3	4860	260	4.7
8	3	2	5040 X	594	11.4
4	3	2	5030 X	592	11.4
2	3	1	4890	514	9.6
3	2	2	4950 X	645	12.3
2	2	2	4970 X	545	10.3
1.5	2	2	4690 X	268	4.9
4	2	1	5020	630	12.0
4	2	1	4960	615	11.7
3	2	1	4930	670	12.7
2	2	1	5010 X	630	12.0
3	2	0.3	-	900	17.6
3	2	0.2	-	1180	23.6
3	1	1	4790 X	422	7.9
3	1	1	4790 X	445	8.3

Consideration of the starred values given shows that in six cases the shock-wave velocities lie between the values 4950 and 5040 m./sec. and do not deviate from a mean value of 5000 m./sec. by significantly more than the anticipated experimental error. It is noteworthy that in these cases the stress values lie within the range $10.3 - 12.3 \times 10^{10}$ dynes/cm.² except in the one case of a 3 in. plate. Of the remaining values two, determined under the same conditions, have a value 4790 m./sec. with associated pressures of 7.9 and 8.3×10^{10} dynes/cm.², while the third with a value 4690 m./sec. corresponds to a pressure of 4.9×10^{10} dynes/cm.². This indicates that the shock-wave velocity decreases with pressure, as is theoretically expected, and hence our measured shock-wave velocities represent a mean value of the actual velocity over the distance measured.

We may compare the cases of attack of 1 in. and 2 in. plates by charges 2 in. long and 2 in. diameter. We will assume that conditions, apart from the plate thickness, are identical in the two cases. We know then that the stress falls by only a small amount, namely, from 12.0 to 10.3×10^{10} dynes/cm.², over the second inch of travel, and may take it to have a mean value of 11.1×10^{10} dynes/cm.² over that distance. If we assume that the mean

velocities do not significantly differ from 5000 m./sec. over both the 1 in. and 2 in. distances, we conclude that the shock-wave velocity at 11.1×10^{10} dynes/cm.² is not significantly different from 5000 m./sec. On the other hand, if we accept our given values exactly, we find that the velocity at this stress is 4940 m./sec. Applying the latter method in a similar way to the cases of attack of 2 in. and 3 in. plates by charges 8 ins. long and 3 ins. diameter, we find that the shock wave velocity at a mean value of 9.6×10^{10} dynes/cm.² is 4870 m./sec. We consider these values to be just significantly greater than the corresponding theoretical ones of 4850 m./sec. and 4790 m./sec. respectively.

We may note also that the experimental velocity of 4790 m./sec. corresponds to a pressure of 8.1×10^{10} dynes/cm.², at which the theoretical velocity is 4750 m./sec., and that when the experimental velocity is 4690 m./sec. the pressure is 4.9×10^{11} dynes/cm.² and theoretical velocity 4650 m./sec. The experiments in which charges 3 ins. long and 2 ins. in diameter were fired against much thinner plates, are included in the table. Unfortunately, in these cases the shock wave velocity can not be calculated with great accuracy because of experimental limitations, but the surface velocity can be obtained and the pressure calculated as described above using the theoretical shock wave velocity. These are included in the table. It can be seen that the pressure in the shock wave falls quite rapidly in the first half inch of travel and is then fairly constant for some distance (fig. 25). It is significant that the first rapid decrease in pressure occurs in the region which shows clear evidence of severe working. It can also be seen why the shock wave velocity seems to be not very dependent on plate thickness since the measured velocity is the mean one given by

$$\bar{U} = \frac{\int_0^T U \, dT}{\int_0^T dT}$$

where T is the distance travelled.

The measurements on the radial variation of surface velocity have shown that in any particular case the initial velocities of all points, in the region measured, are the same. In these cases, therefore, we may conclude that the shock-wave amplitude is constant over radial distances of at least 1.25 in. The subsequent velocity changes associated with curvature of the scab in this region are undoubtedly a result of the processes occurring nearer to and at the scab edge, where there must be a surface velocity gradient. The fracturing of the scab edge, and also any extension of the primary fracture which might be involved, both require energy which must be withdrawn from the energy trapped in the scab by the primary scabbing process. Hence the final velocity, after it becomes completely detached, will be determined by these effects as well as by the amount of energy initially trapped. If the amount of work required to produce the fractures is greater than this energy, then the scab will not completely separate from the plate, as shown in fig. 18a. On the other hand, the work required is clearly related to the scab circumference, and if we could find a way of concentrating into a smaller region the energy supplied by the explosive to the plate, we should succeed in producing a smaller scab and probably a given charge would then be able to cause a scab to be detached from a thicker plate. Some kind of wave-shaping might be effective in this respect.

When a scab finally becomes detached from a plate, every point on it must move with the same velocity, so that at some stage during its formation it seems probable that points near the edge will be accelerated at the expense of energy from the centre part of the scab. The behaviour of the curves peculiar to the C points of the 3 in. plates may be attributable to this effect.

We are not aware of any previous measurement of scab thickness which showed that this quantity can vary considerably along the scab radius (i.e. perpendicular to the charge axis). This is probably due to the fact that most of the previous work on scabbing has involved charge diameters not much greater than the plate thickness. Under these conditions it is true to say that the scab thickness is fairly uniform. On the other hand, as figs. 18 to 23 clearly show, scab thickness is in general by no means uniform.

We have seen that the scab thickness is a measure of the initial slope of the stress displacement curve behind the shock front. Knowing the amplitude at the front, we may therefore construct the first part of the stress displacement curve, in any particular case, along a line through the steel parallel with the charge axis and at a time corresponding to the moment of reflection. By the term "first part" we mean over a distance equal to twice the scab thickness taken along the line. The curve so constructed will not exactly represent physical conditions owing to the several assumptions implicit in the method of drawing it, but it must have real qualitative significance. Hence it is useful to construct and compare such curves along a charge axis for two thicknesses of plate attacked by similar charges. Fig. 26 shows the result of the construction for the case of the attack of 1 in. and 2 ins. plates by charges 2 ins. long and 2 ins. diameter, thereby indicating the general change in shape of a given stress wave as it proceeds further into the steel. We assume the same shaped wave front as previously for the sake of consistency, and using the values given for stress and scab thickness in Tables IX and VII, we then plot the stress curves back to a distance from the front equal to twice the scab thickness. Recalling the work of Hill and Pack (16), we expect the axial pressure about 1 in. behind the detonation front to be, in our case, about one third of the peak pressure. Our measurements on the shock wave would suggest by themselves that the initial pressure in the shock wave is of the order of 30×10^{10} dynes/cm.². This figure is in quite good agreement with that of 28.3×10^{10} dynes/cm.² quoted by Pack, Evans and James (9) and obtained from the detonation pressure of plastic explosive (16.3×10^{10} dynes/cm.²). Thus the pressure 1 in. behind the detonation front is about 5×10^{10} dynes/cm.². Since the sonic velocity in the explosive and the shock wave velocity are not greatly different we may assume, for this very qualitative treatment, that when the shock front has travelled 1 in. into the steel plate, the pressure at the interface will have fallen to about 9×10^{10} dynes/cm.²; by similar reasoning it is found that when the shock wave has travelled 2 ins. into the steel plate the pressure at the interface will have dropped to about 2×10^{10} dynes/cm.². Using these values approximate stress-time curves have been sketched in fig. 26. The third curve in fig. 26 was obtained for a charge 3 ins. diameter and 2 ins. long against a plate 3 ins. thick. The results are not directly comparable but give an indication of the change in shape of the stress-time curve.

It has been pointed out above that unloading will take place in the steel plate in a direction at right angles to the direction of propagation of the shock wave. Clearly, the unloading effect will increase as the ratio of charge diameter to plate thickness decreases. At the scab edge it is reasonable to assume that unloading effects are almost independent of this last ratio and are independent also of the charge length. We find, in fact, that the scab thickness at the edge is almost constant for a given plate thickness. The results also imply that the slope, behind the shock front at the scab edge, decreases with increasing distance travelled. Further, we expect the scab thickness at the centre to be dependent both on the charge diameter to plate thickness ratio and on the charge length up to the value for which it becomes effectively infinite. Our results confirm these expectations, and it is interesting to note that when these two values tend to the minimum required for any scabbing at all, so that unloading effects due to both the finite length of the charge and the lateral unloading in the plate become a maximum, then the scab thickness at the centre tends to a minimum value equal to the thickness at the edge. This type of unloading in which the unloading wave moves faster than, and so attenuates, the shock front, is to be

contrasted with the unloading of the detonation wave in which the unloading wave travels with a velocity determined by the sonic velocity in the detonation products according to the Chapman-Jouget condition and which is not greater than the detonation velocity.

We have neglected any effect due to reflection of the elastic part of the wave front. Since its amplitude is maintained it must alter the stresses behind the front all by the same amount and will not therefore alter the slope of the curve, so that our previous conclusions hold good. Further, owing to its small amplitude, it seems unlikely that the reflection of the elastic front alone could ever lead to the formation of a fracture surface.

Finally, we may say something about the other fractures observed in the plate. We have to remember that the total variation with time of the stress-pattern in the plate is complicated not only by the primary reflection of the free surface but also by both the fracture process and subsequent multiple reflections from the plate boundaries. On the other hand, the rate of attenuation of the shock wave is probably sufficient to make any reflection of the tension wave from the explosive steel interface of little effect on the fracture pattern. The most important effect will probably be at the initial fracture surface, since in many cases the material behind this surface will still be highly stressed after the moment of fracture. The fracture process itself will undoubtedly contribute to the relief of this stress, but it is likely that reflection of the first type will occur at the new surface and further scabbing surfaces be obtained. Such an effect would explain the second scabbing surface, which is particularly evident in fig. 23b and developed to some extent in other cases; it would also account for the loss of layers of metal not associated with the main scab, particularly noticed at the centre of the scab region.

The 1 in. plates attacked by charges 3 in. diameter are exceptional in giving a hole punched right through. The edge of this hole appears to be the result of a shearing fracture, and the complications introduced by this effect might be the cause of the scabbing surfaces which are observed in these cases. In every other case fracture surfaces are not observed within the primary scab, and a consideration of the scabbing mechanism shows that such a fracture cannot be expected. If, as is probable in these exceptional cases, the conditions for scabbing have not been attained by the time the reflected tension wave has reached the explosive steel interface, then this wave will be strongly reflected as a compression wave and can subsequently cause scabbing at the other surface. Under these circumstances the nature of the scab will be different from that where scabbing is a direct result of the first stress reflection.

The above discussion presents little more than qualitative views, but is in agreement with available theoretical data on stresses and shock waves surprisingly good and does suggest that a more thorough and detailed study might produce some very useful information about the equation of state of solids and the conditions within the detonation wave.

The general scab characteristics are generally in agreement with the accepted theories of shock wave propagation; they agree very roughly with some of the empirical rules that have been suggested. It is clear that the critical ratio of charge diameter to plate thickness for scabbing is due to lateral unloading in the plate, but it is difficult to see how this can be prevented. In some cases lateral fractures are present without the scab having been fully detached; this is because the scab energy has been completely expended in fracturing steel before the scab is finally separated. Clearly, the energy required to separate the scab depends on the scab circumference, and it would seem therefore that a given charge would be able to scab a greater thickness of steel if the energy could be concentrated into a smaller area so as to produce a smaller scab. Some use of the detonation wave might help to achieve this. It must, however, be remembered that the price of using a wave-shaper is that the part of the explosive in contact with the plate will be of lower power than that now used, and also that it may be very difficult to make a wave-shaper function satisfactorily in the squash-head projectile.

6. Conclusions

(1) The average velocity of the shock wave produced by plastic explosive detonated in contact with mild steel plate 1 to 3 ins. thick is very close to 5000 m./sec. and only slightly dependent on plate thickness. The velocity is, however, probably greater in the first $1/4$ - $1/2$ in. of travel. The velocities obtained are in good agreement with those calculated from the Rankine-Hugoniot equations together with an equation of state for steel.

(2) Displacement-time curves of the plate surface up to about 0.4 ins. have been obtained for plates attacked by a wide range of charge sizes. Most of the curves are continuous except near to the plate, where there is evidence of the wave of elastic deformation. With long charges most of the curves have constant slope, but as the charge length decreases the slope tends to decrease with displacement. The face velocity increases with charge length up to a length-diameter ratio of 2 and decreases with plate thickness.

(3) The particle velocity and shock wave stress calculated from the surface velocity are in reasonable agreement with theory and give a qualitative picture of the shape of the stress-time curve in the steel. The stress decreases rapidly in the first $1/4$ - $1/2$ in. of metal, is then fairly constant for about 1-2 ins., and finally decreases fairly rapidly to below the yield stress.

(4) The scab diameter is approximately 1.5 times the charge diameter but does tend to increase with plate thickness.

(5) The thickness of the scab at the edge is constant for a given plate thickness and roughly proportional to plate thickness. The thickness of the scab at the centre is dependent on the ratio of plate thickness to charge diameter; if the ratio is unity the scab thickness is more or less uniform, but with thinner plates the scab is much thicker in the centre. The variations in scab thickness agree with a simple qualitative theory of shock wave interaction assuming changes in the stress-time curves caused by lateral unloading waves.

(6) The limiting thickness of plate that can be scabbed by a given charge is governed by lateral unloading. Many charges give a lateral scabbing fracture but the scab contains insufficient energy to detach itself from the plate. The only obvious method of increasing the efficiency of scabbing is to concentrate the same amount of energy into a smaller scab by modification of the detonation wave shape. It would be worthwhile to investigate the effect of wave-shaping, although it is doubtful whether this could be incorporated in a squash-head weapon in its present form.

7. Bibliography

Page No.

- (1) Symposium on Penetration of Armour, Part III.
Ministry of Supply September, 1948. 1
- (2) J. U. Woolcock. C.E.A.D. Technical Reports
33/44, 19/45, 8/47, 8/52. 1
- (3) B. Hopkinson. Proc. Roy. Soc.
A.213,437 (1914). 1
- (4) J. W. Landon. Proc. Roy. Soc.
A.103,622 (1923) 1
- (5) R. M. Davies. Trans. Roy. Soc.
A.240,375 (1948) 1
- (6) J. S. Rinehart. J. Appl. Phys.
22,555 (1951) 2
- (7) J. S. Rinehart. J. Appl. Phys.
22,1178 (1951) 2
- (8) D. E. Edwards. F.V.D.E. Report M.25A.
September, 1951. 3
- (9) D. C. Pack, W. M. Evans and H. J. James. Proc. Phys. Soc.
60,1 (1948) 4
- (10) Hughes, Pondrom and Mims. Phys. Rev.
75,152 (1949) 4
- (11) R. D. Fay and O. V. Vortier, J. Acous. Soc. Am.
23,339 (1951) 4
- (12) P. W. Bridgman.. The Physics of High Pressures, London, 1931.
- (13) P. W. Bridgman. Phys. Rev.
57,235 (1940) 4
- (14) T. von Karman and P. Duwez. J. Appl. Phys.
21,897 (1950)
- (15) OSRD Report 15-140-75A, SR7/4827. 6
- (16) R. Hill and D. C. Pack. Proc. Roy. Soc.
A.191,524 (1947) 6
- (17) F. Chorlton. A.D.E. Report 4/52
June, 1952. 6
- (18) H. F. Bohnenblust. OSRD 781, SR7/2729 6
- (19) R. H. Cole. Underwater Explosions, p.64 et seq. Princeton
University Press, 1948. 13
- (20) F. I. Hill. B.R.L. Memo. Report No. 519a.
December, 1950. 3

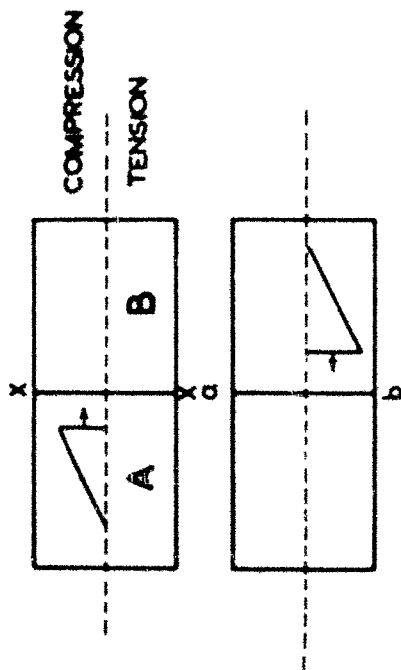


FIG. 1.

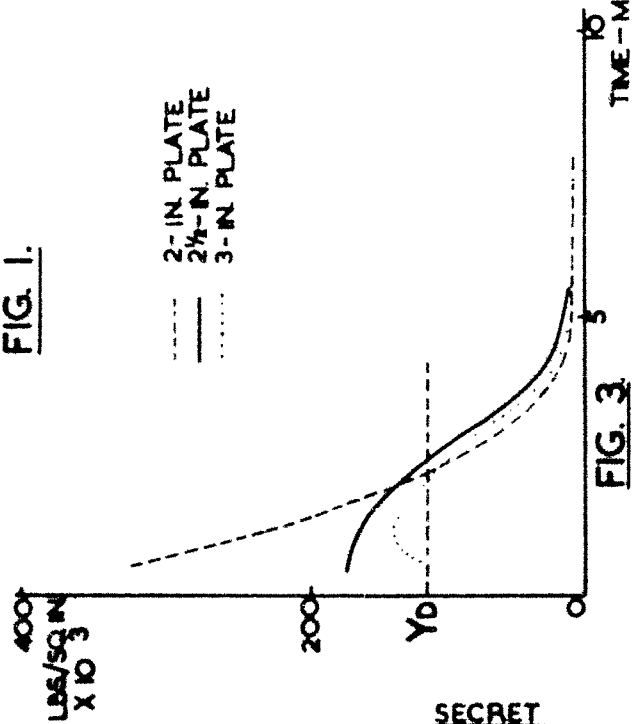


FIG. 3.

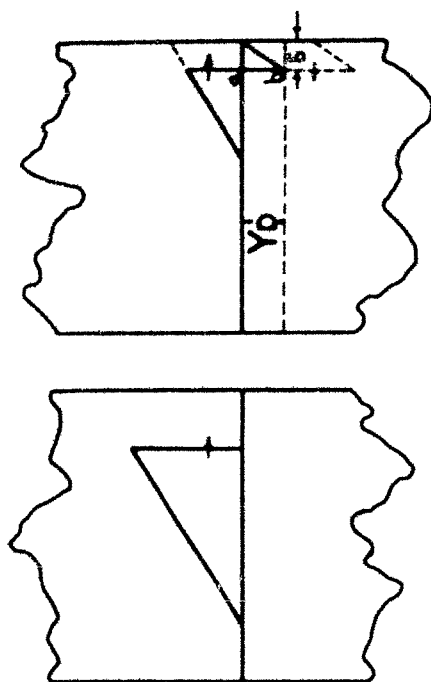


FIG. 2.

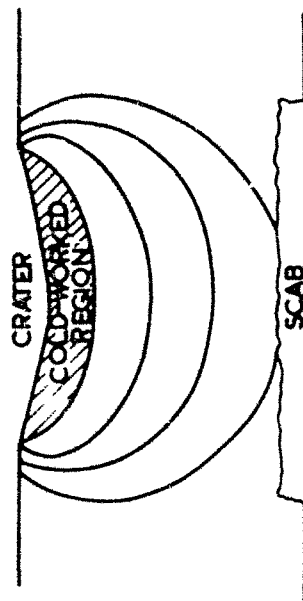


FIG. 4.

SECRET

SECRET

SECRET

THEORETICAL SHOCKWAVE VELOCITY
AGAINST PRESSURE.

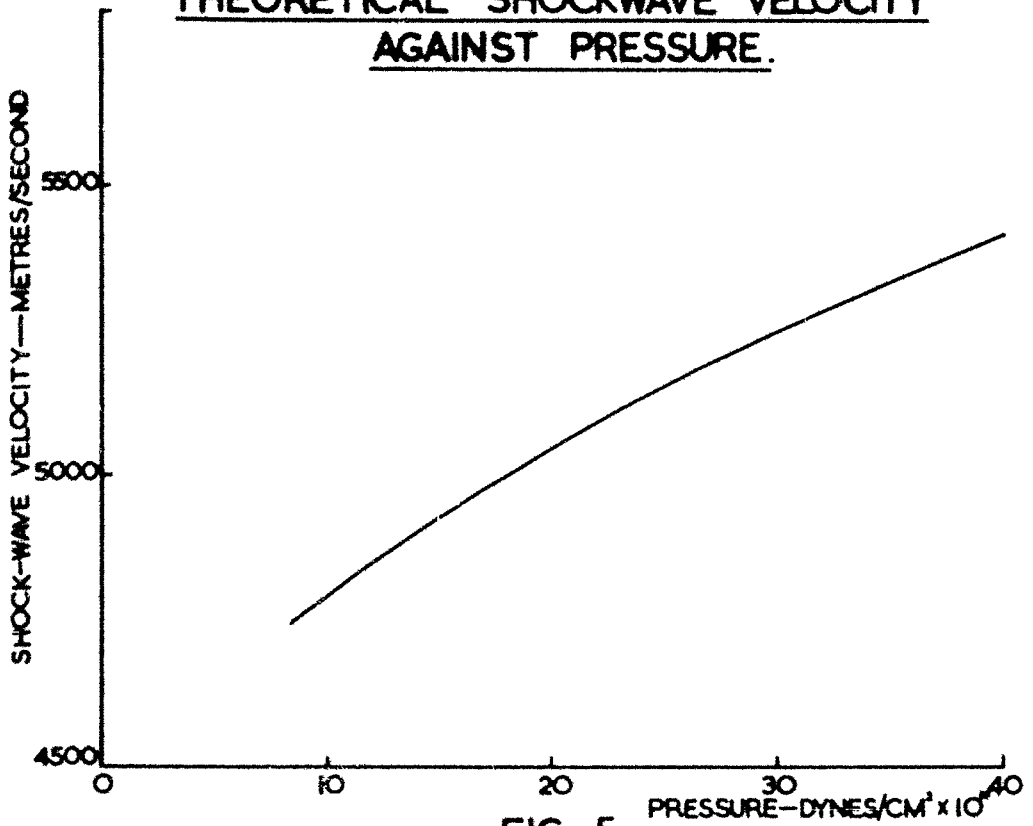


FIG. 5.

HYPOTHETICAL PRESSURE DISPLACEMENT
CURVE.

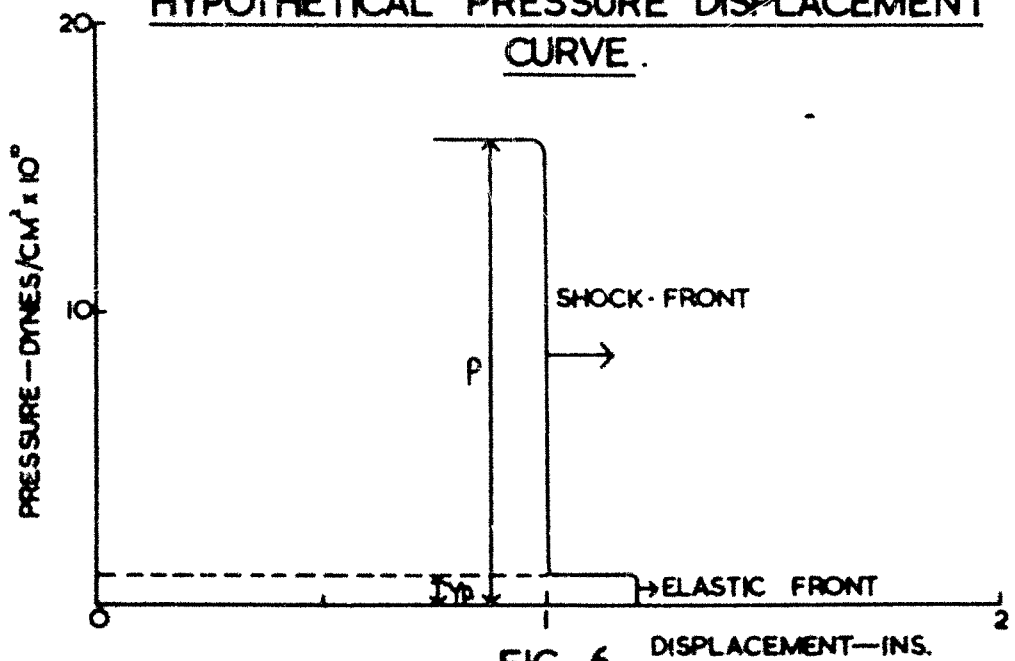


FIG. 6.

SECRET

PRESSURE BEHIND DETONATION FRONT IN BLOCK OF T.N.T. 2 CMS. THICK.

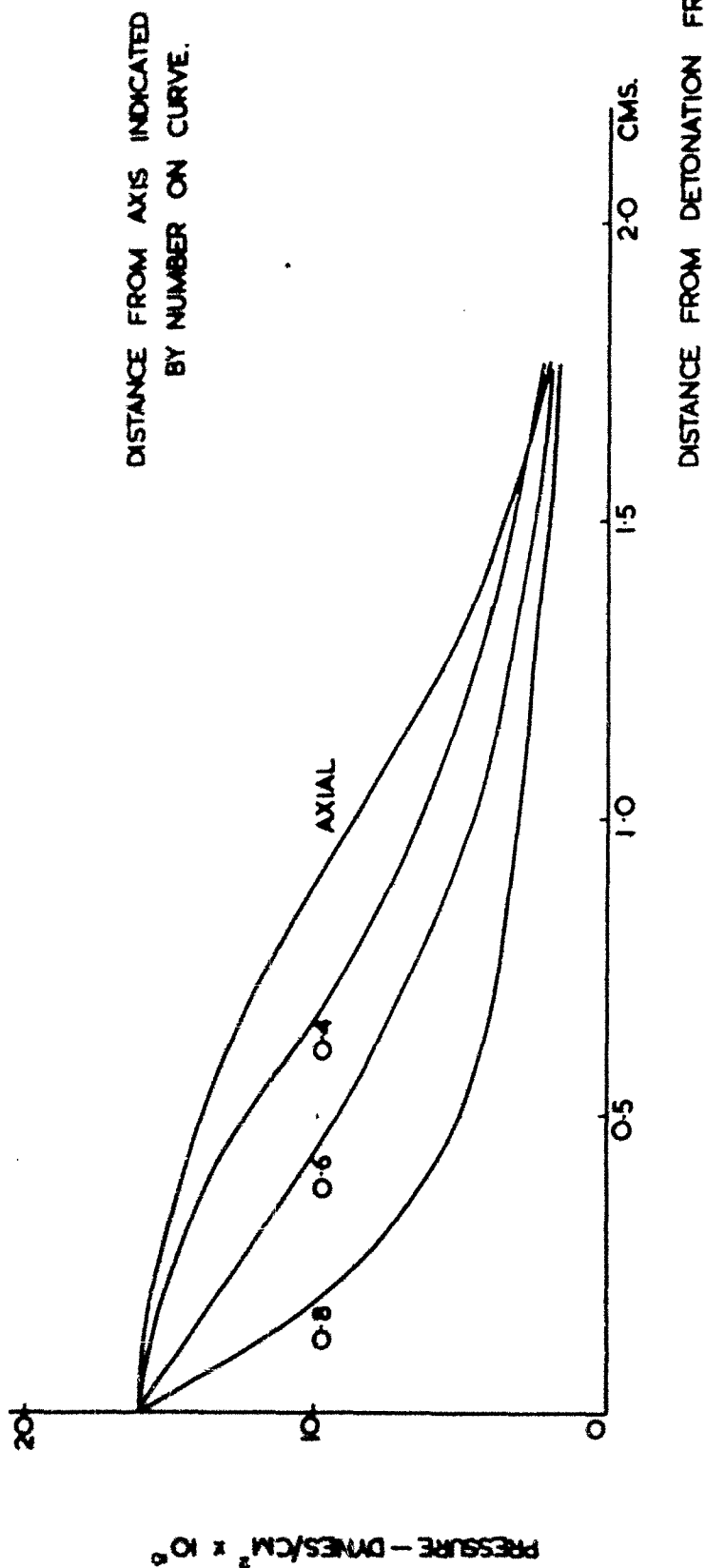


FIG. 7

SECRET

SECRET

SECRET.

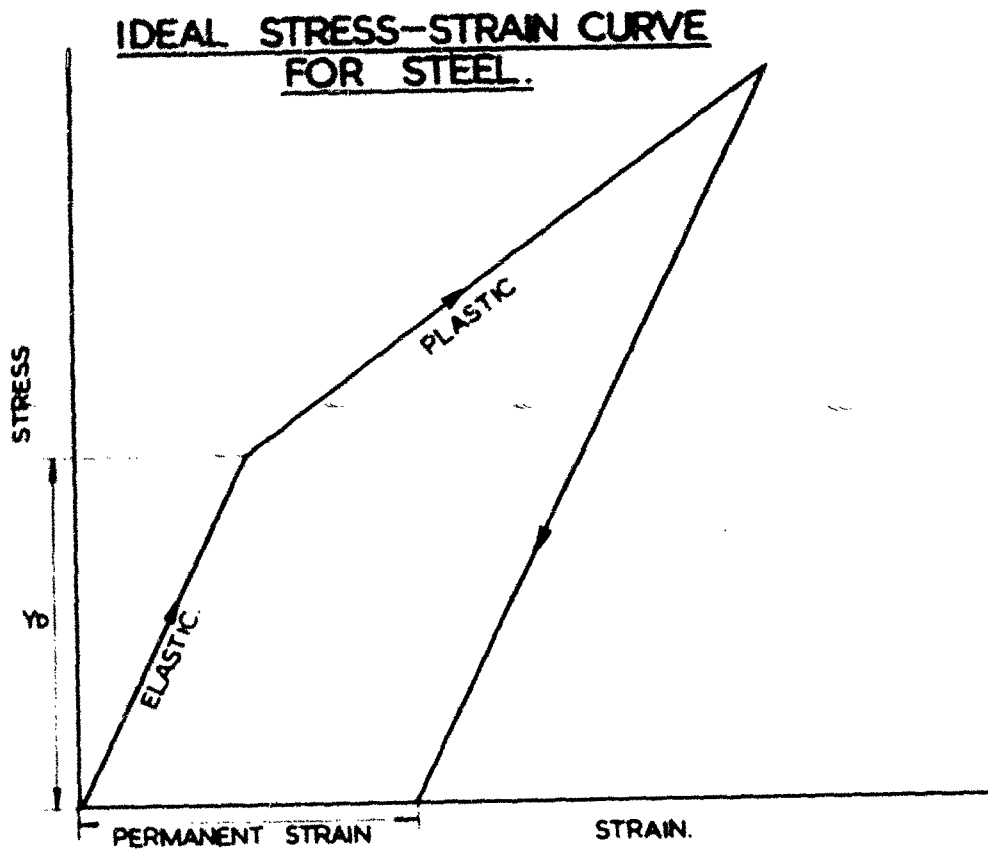


FIG. 8

EVENT CIRCUIT.

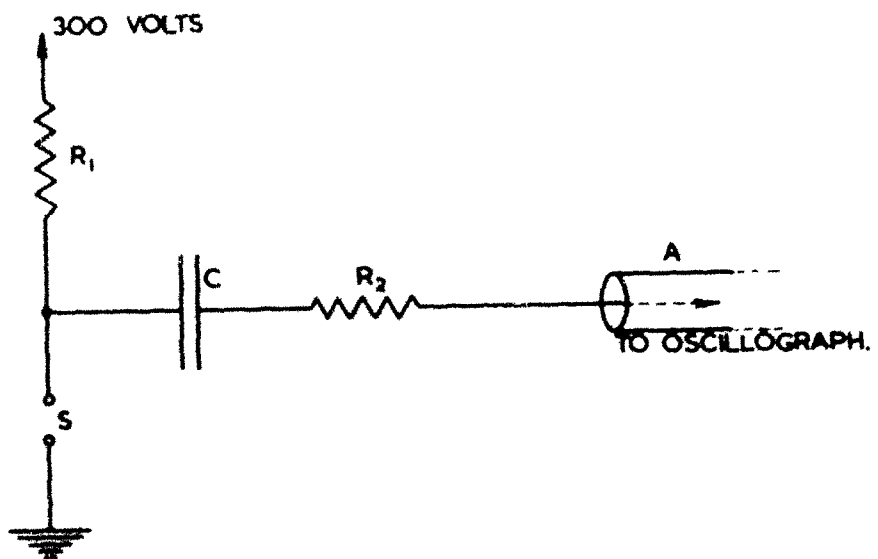
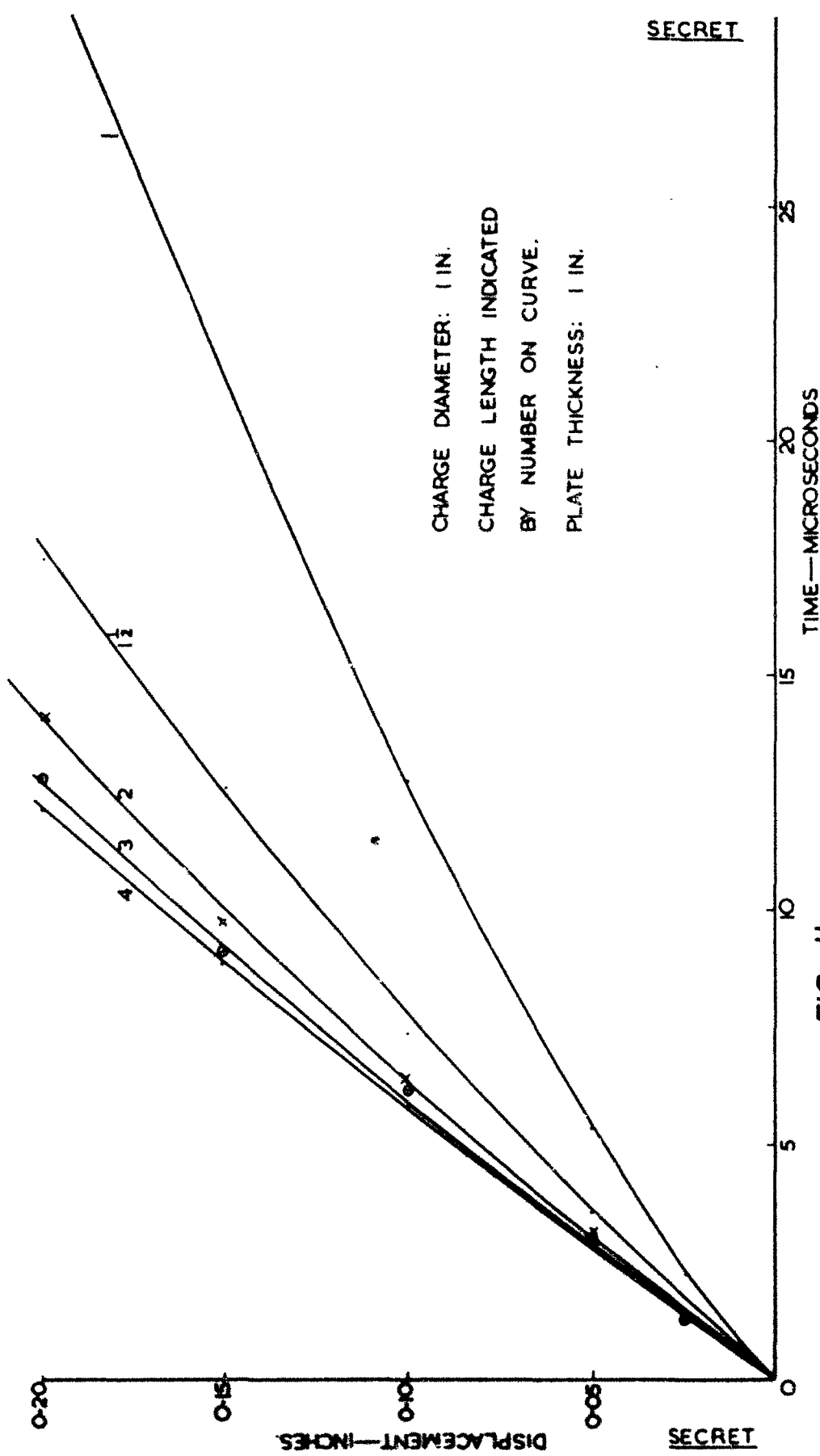


FIG. 9

SECRET.

SECRET



CHARGE DIAMETER: 1 IN.
CHARGE LENGTH INDICATED
BY NUMBER ON CURVE.
PLATE THICKNESS: 1 IN.

FIG. II.

SECRET

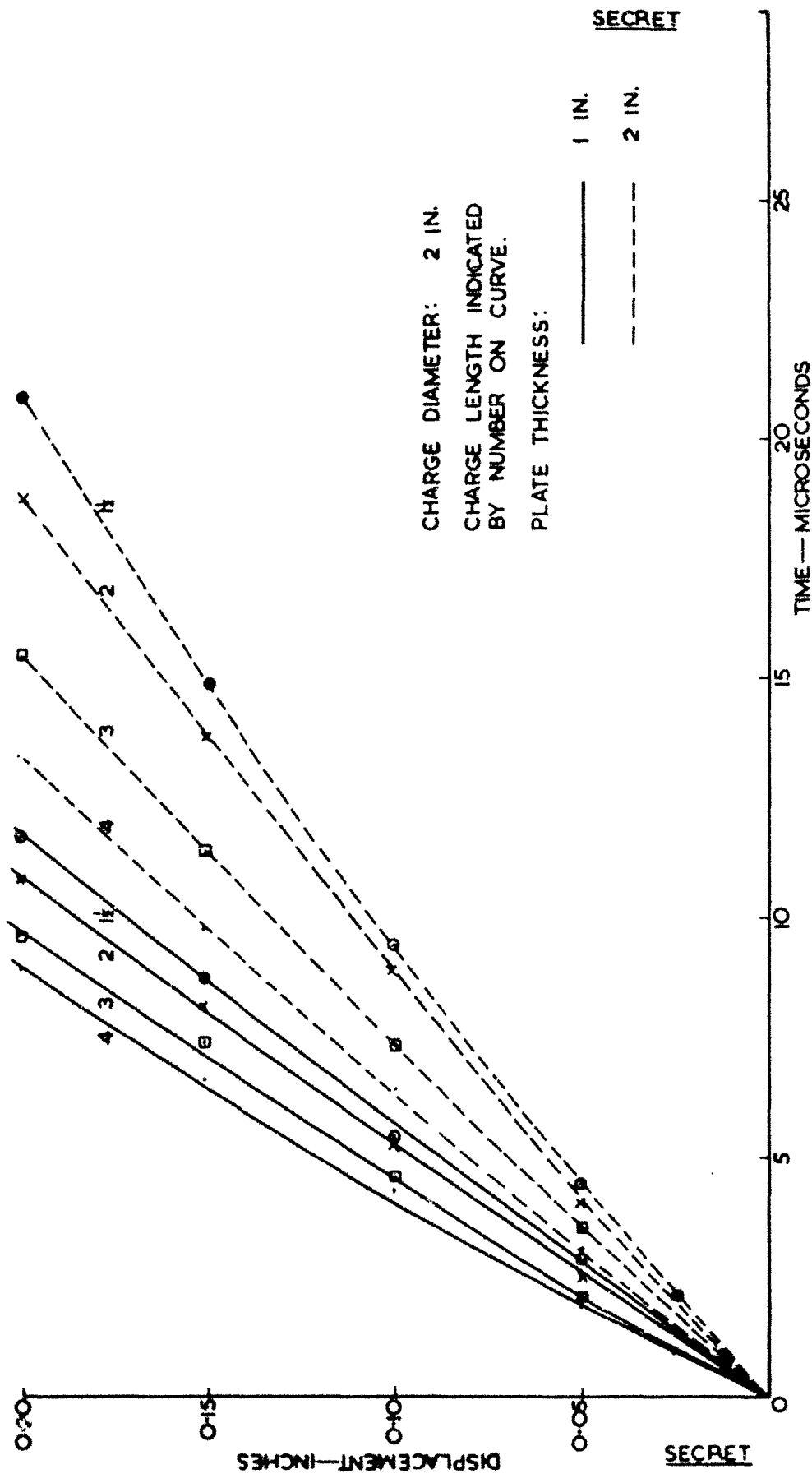


FIG. 12.

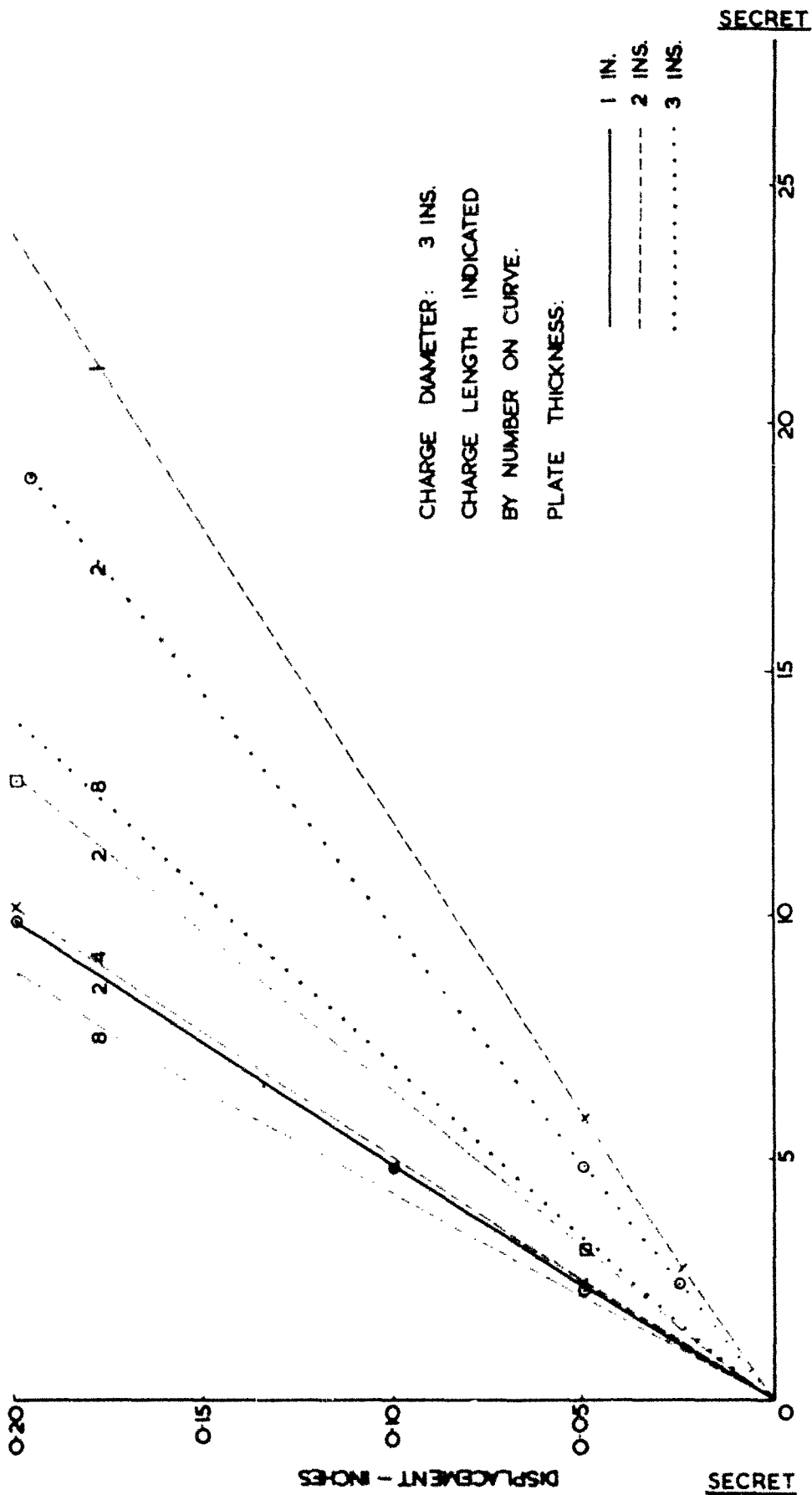


FIG. 13.

SECRET

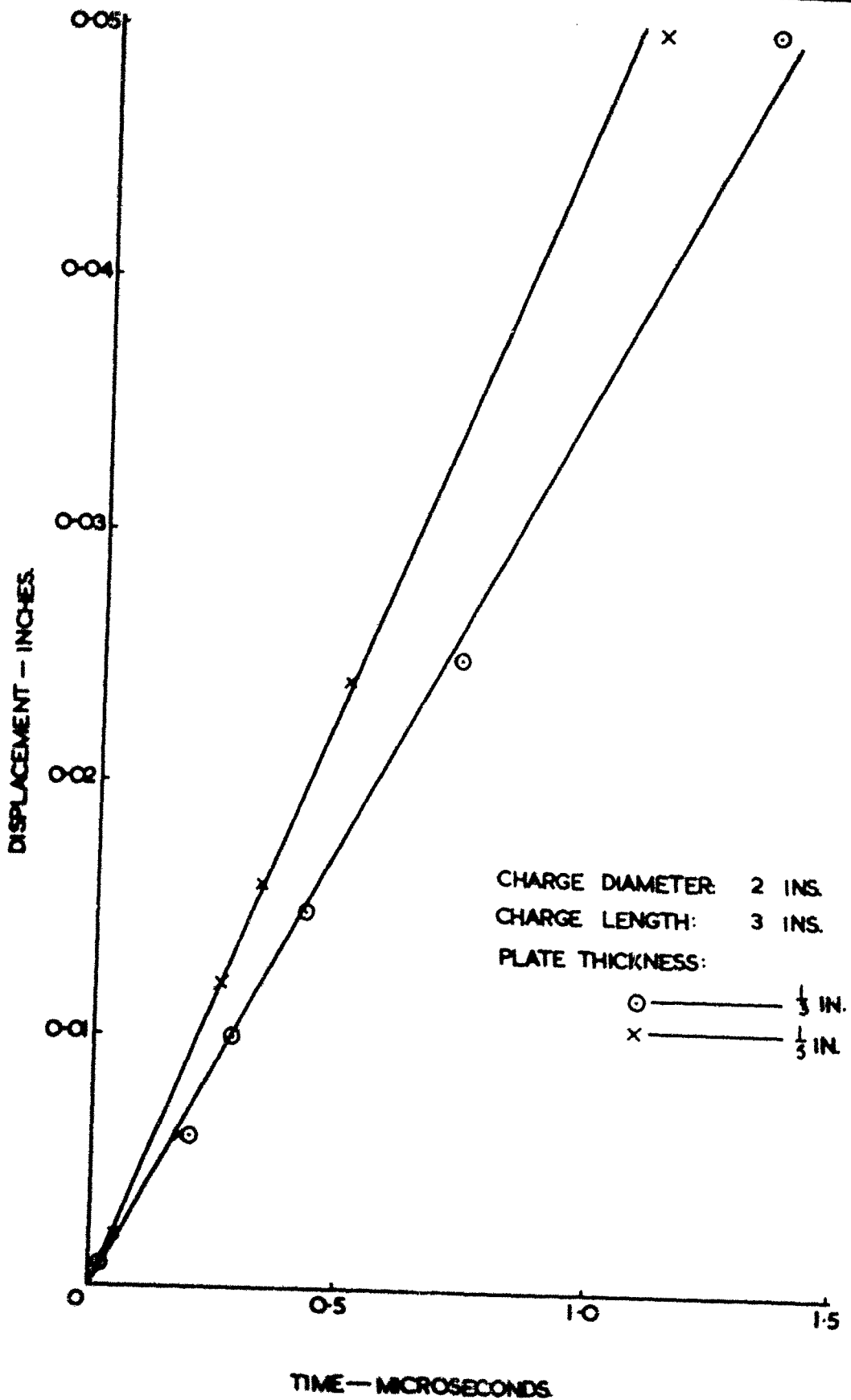


FIG. 14.

SECRET

SECRET

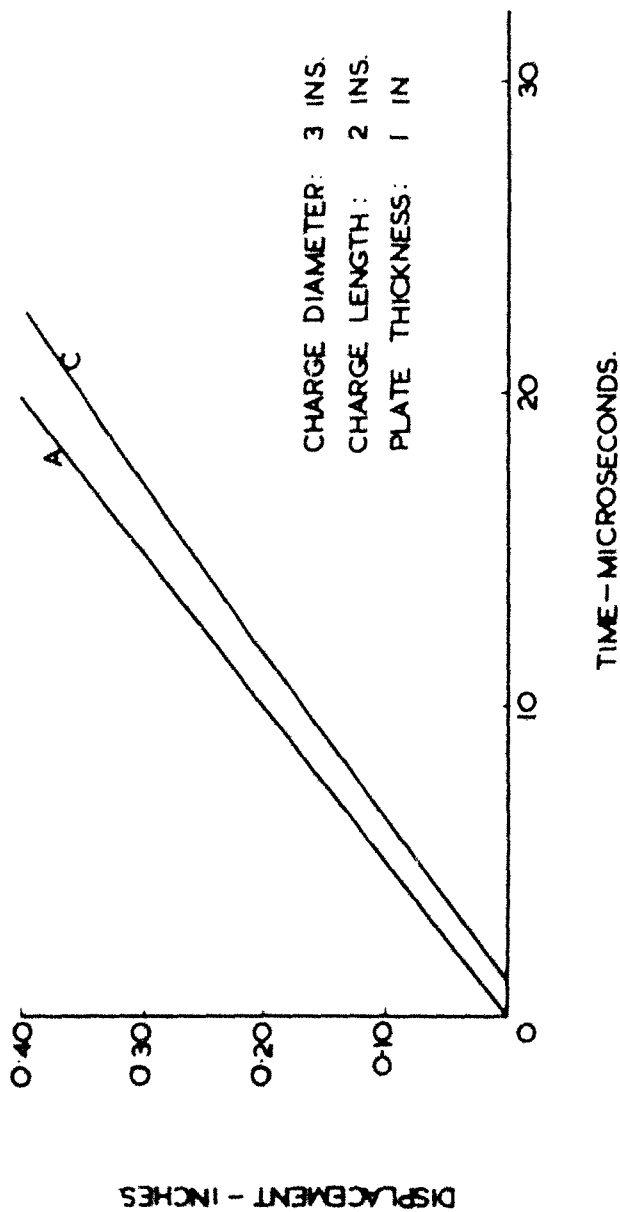


FIG. 15.

SECRET

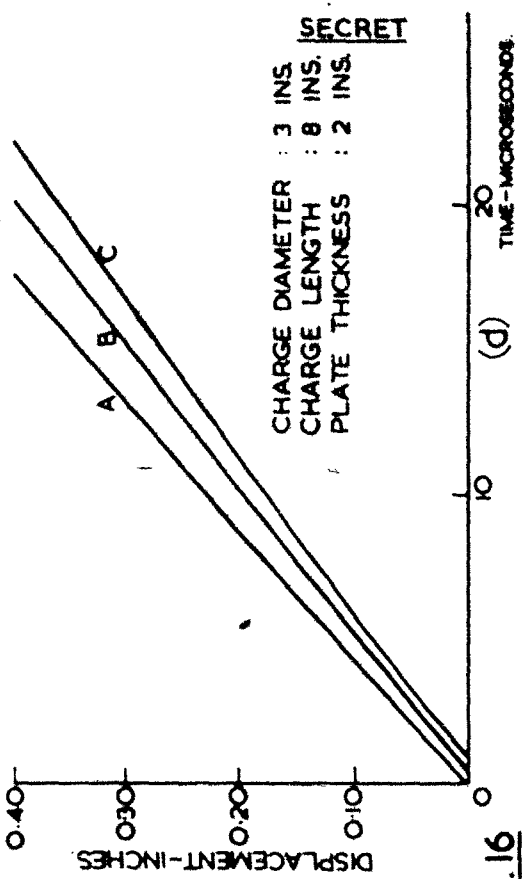
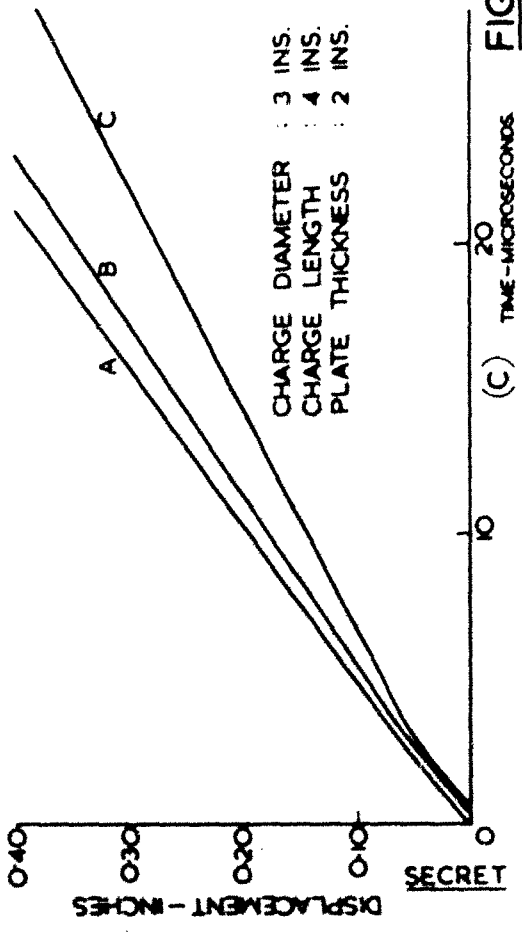
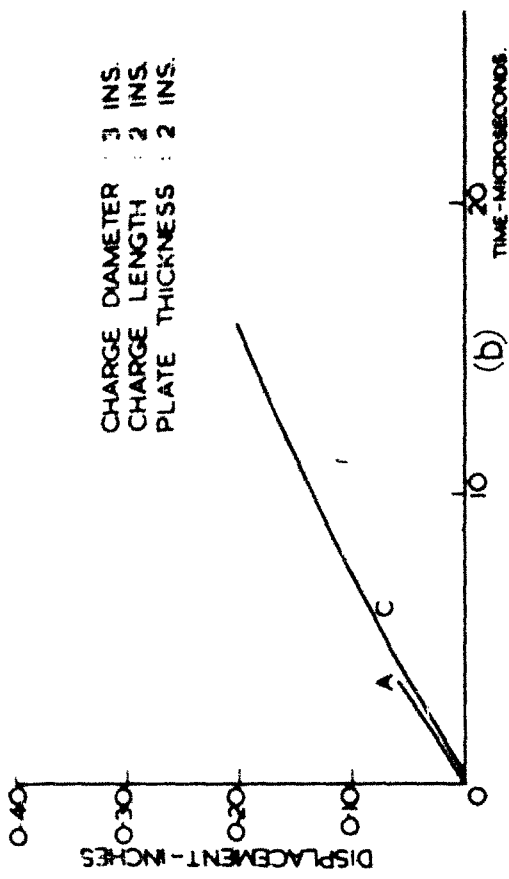
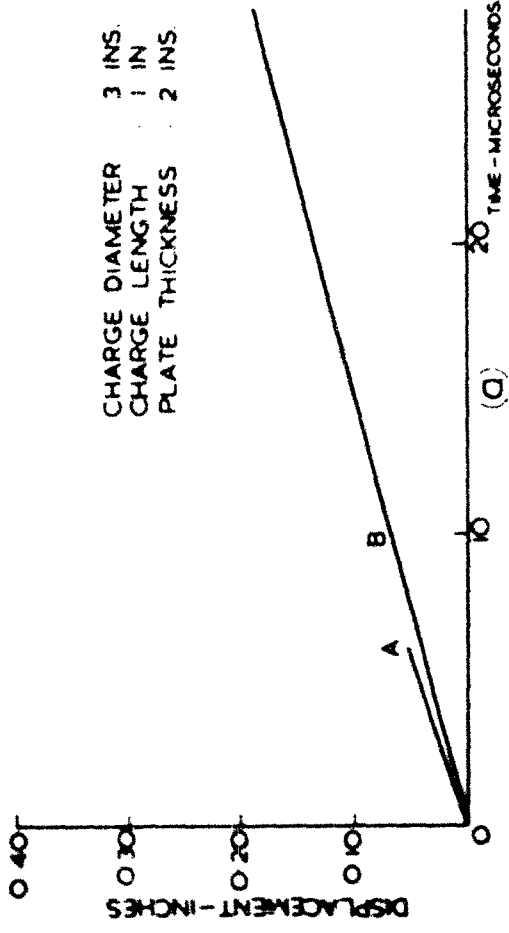
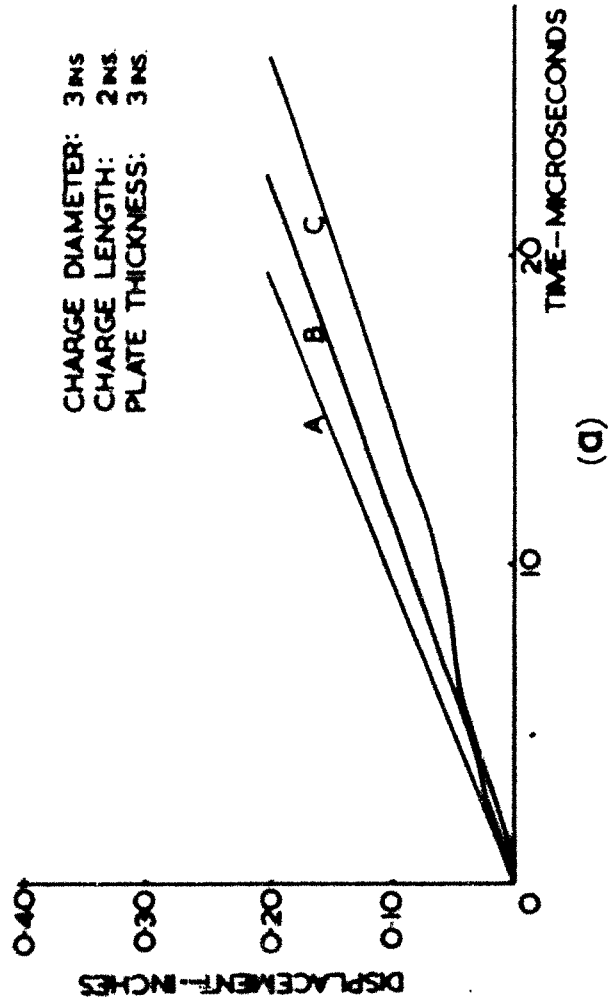


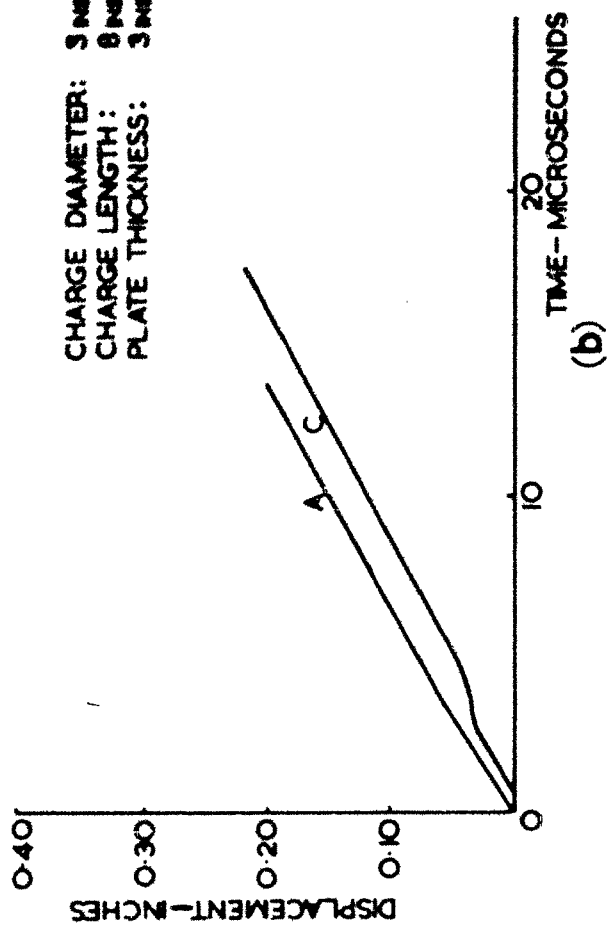
FIG. 16

SECRET

SECRET



SECRET



SECRET

FIG. 17

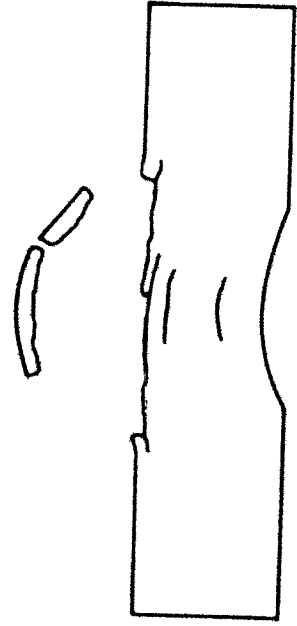
1 IN. DIAMETER CHARGE. 1 IN. THICK PLATE.

SECRET



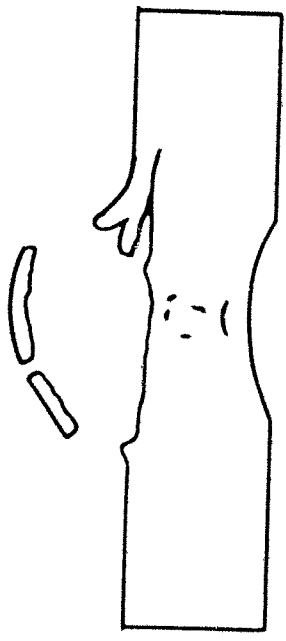
(a)

CHARGE LENGTH. 1 IN.



(b)

CHARGE LENGTH. 1.5 IN.



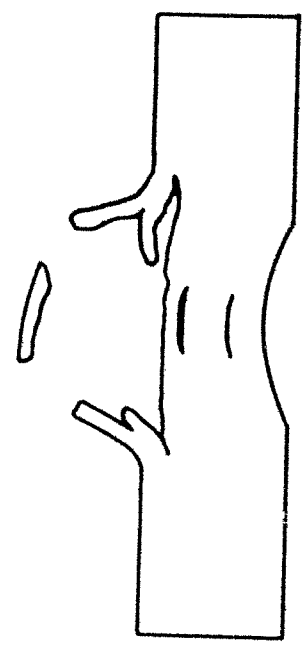
(c)

CHARGE LENGTH. 2 IN.



(d)

CHARGE LENGTH. 3 IN.



(e)

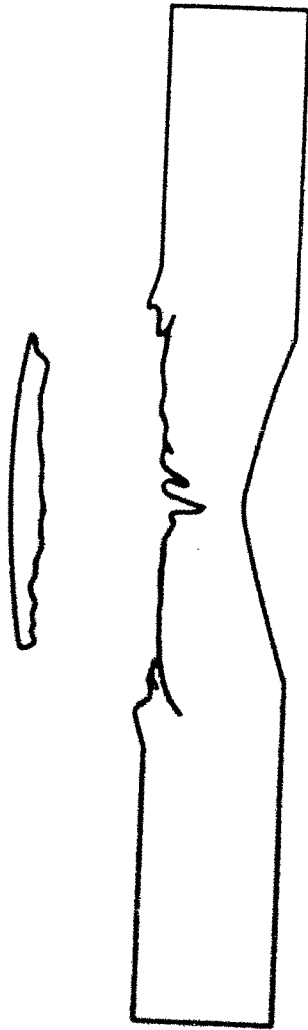
CHARGE LENGTH. 4 IN.

FIG. 18

SECRET

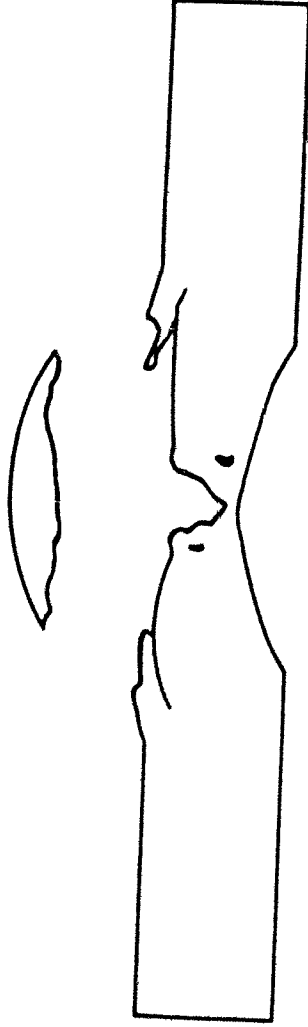
2 IN. DIAMETER CHARGE. 1 IN. THICK PLATE

SECRET



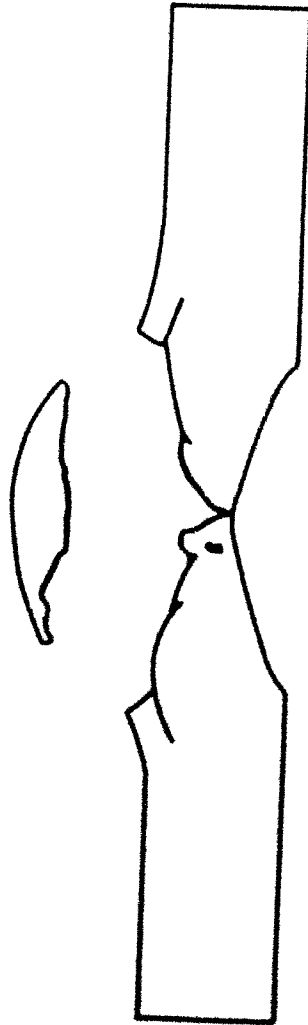
(a)

CHARGE LENGTH 15 IN.



(b)

CHARGE LENGTH 2 IN.



(c)

CHARGE LENGTH 3 IN.



(d)

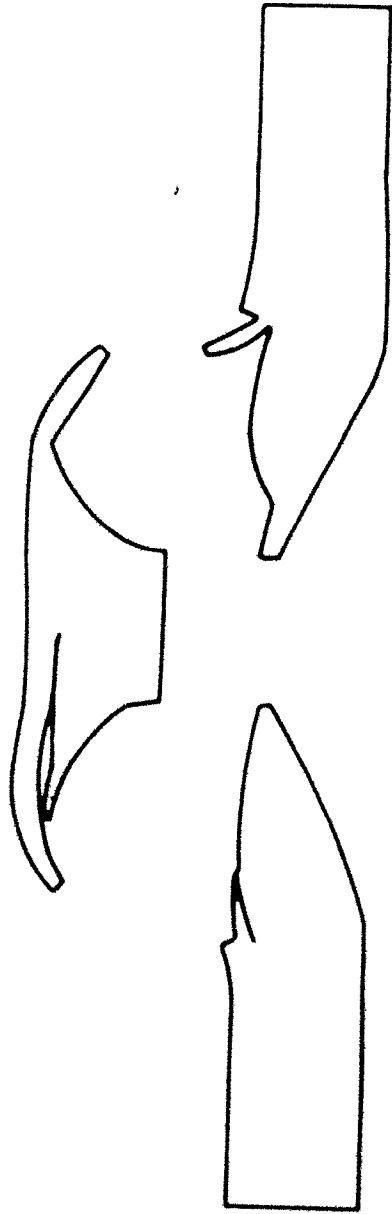
CHARGE LENGTH 4 IN.

FIG. 19

SECRET

3 IN. DIAMETER CHARGE. 1 IN. THICK PLATE.

SECRET



(a)

CHARGE LENGTH. 1 IN.



(b)

CHARGE LENGTH. 2 IN.



(c)

CHARGE LENGTH. 4 IN.

FIG. 20.

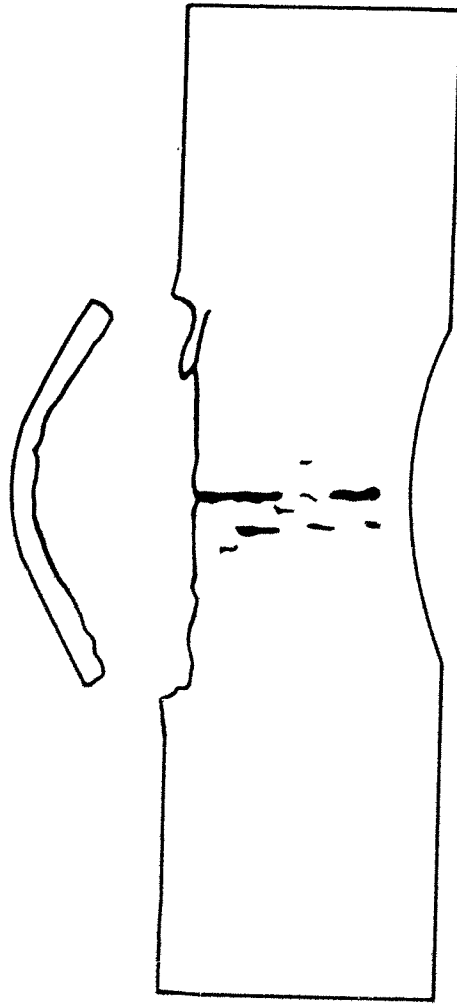
2 IN. DIAMETER CHARGE. 2 IN. THICK PLATE.

SECRET



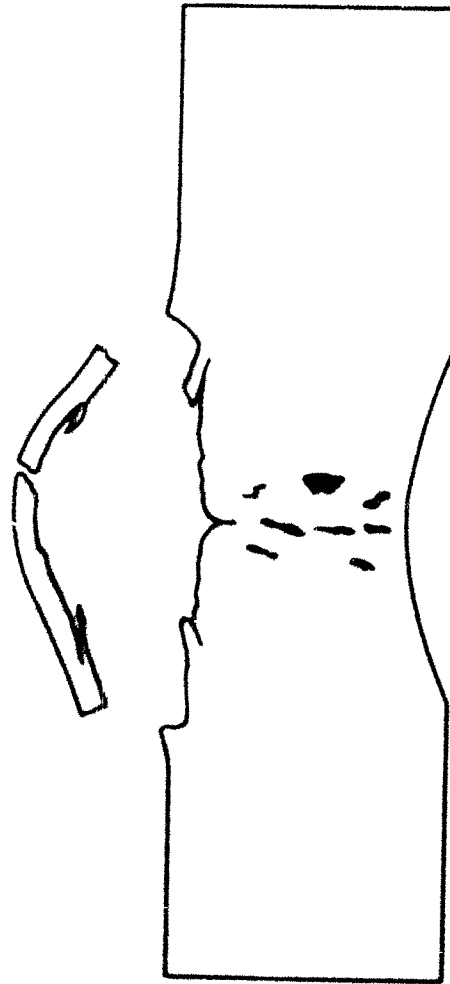
(a)

CHARGE LENGTH 1.5 IN.



(b)

CHARGE LENGTH 2 IN.



(c)

CHARGE LENGTH 3 IN.



(d)

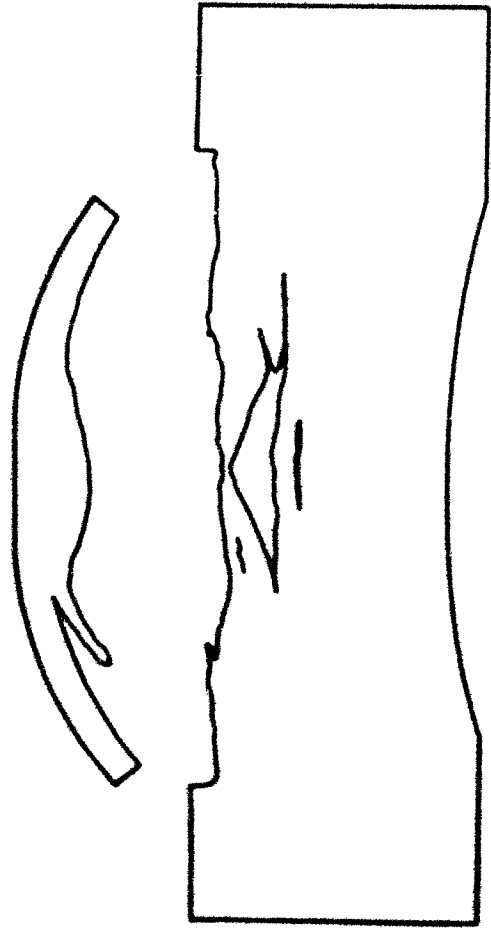
CHARGE LENGTH 4 IN.

FIG. 21.

SECRET

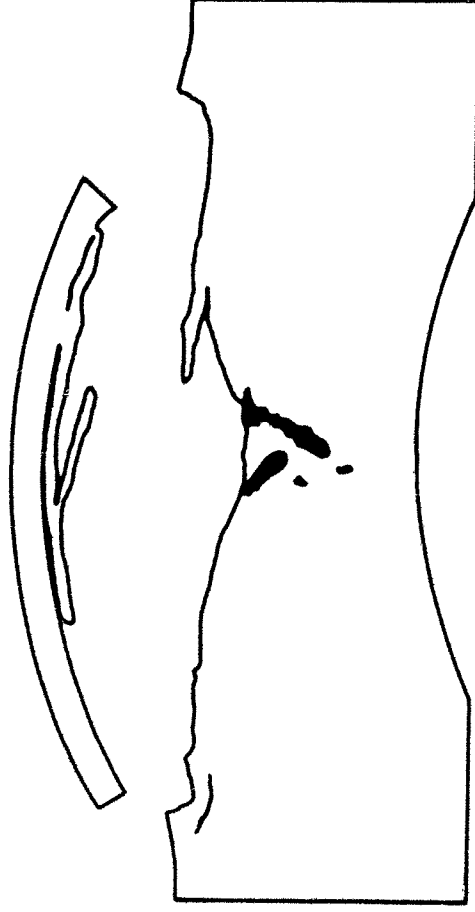
3. IN DIAMETER CHARGE. 2 IN. THICK PLATE.

SECRET



(a)

CHARGE LENGTH 1 IN.



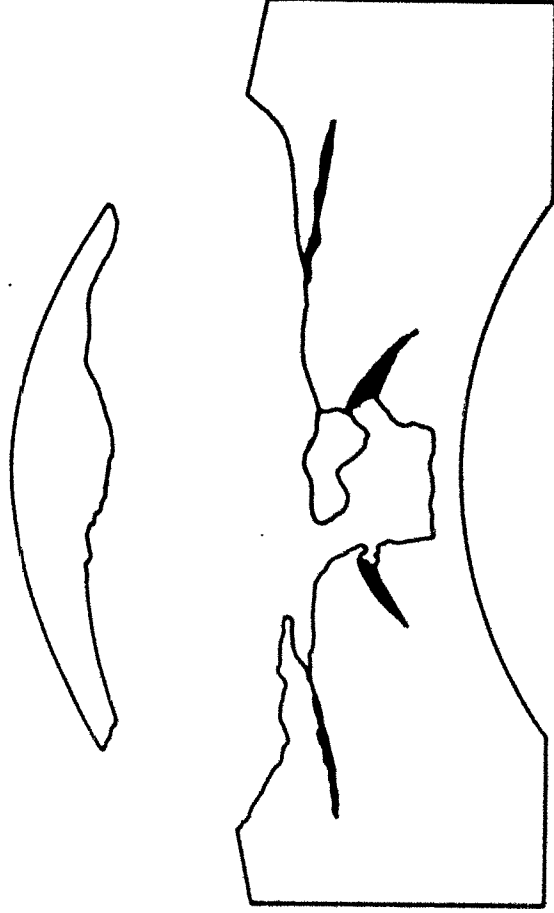
(b)

CHARGE LENGTH 2 IN.



(c)

CHARGE LENGTH 4 IN.



(d)

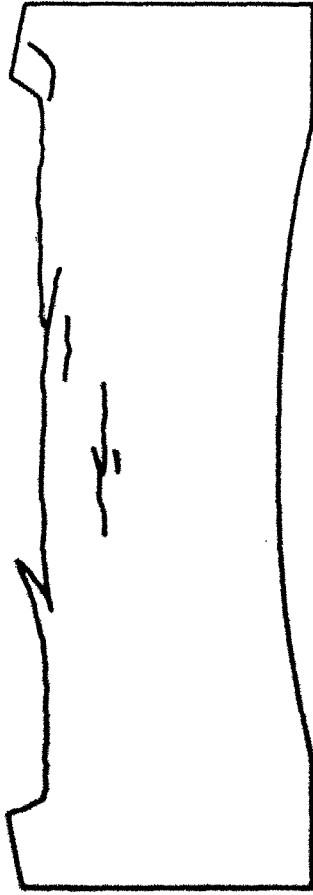
CHARGE LENGTH 6 IN.

FIG. 22.

SECRET

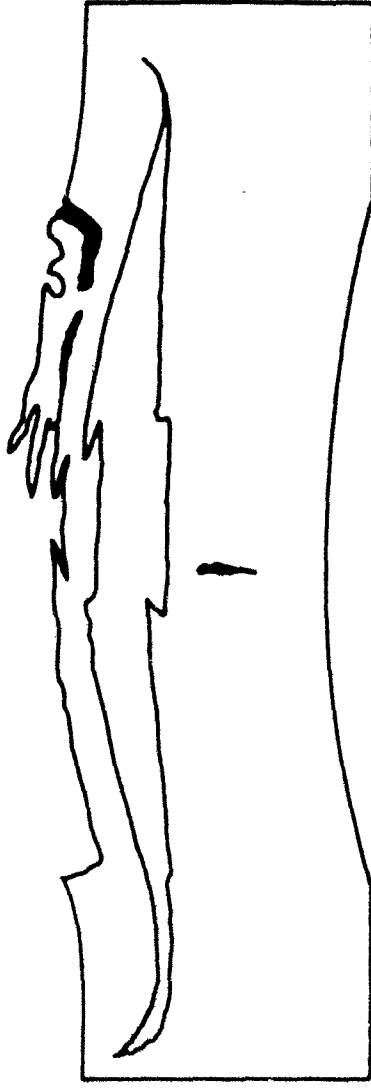
3. IN DIAMETER CHARGE 3 IN. THICK COMPOSITE PLATE.

SECRET



(a)

CHARGE LENGTH. 2 IN.



(b)

CHARGE LENGTH. 8 IN.

FIG. 23.

SECRET

SECRET

HYPOTHETICAL DISPLACEMENT TIME CURVE
FOR PLATE SURFACE

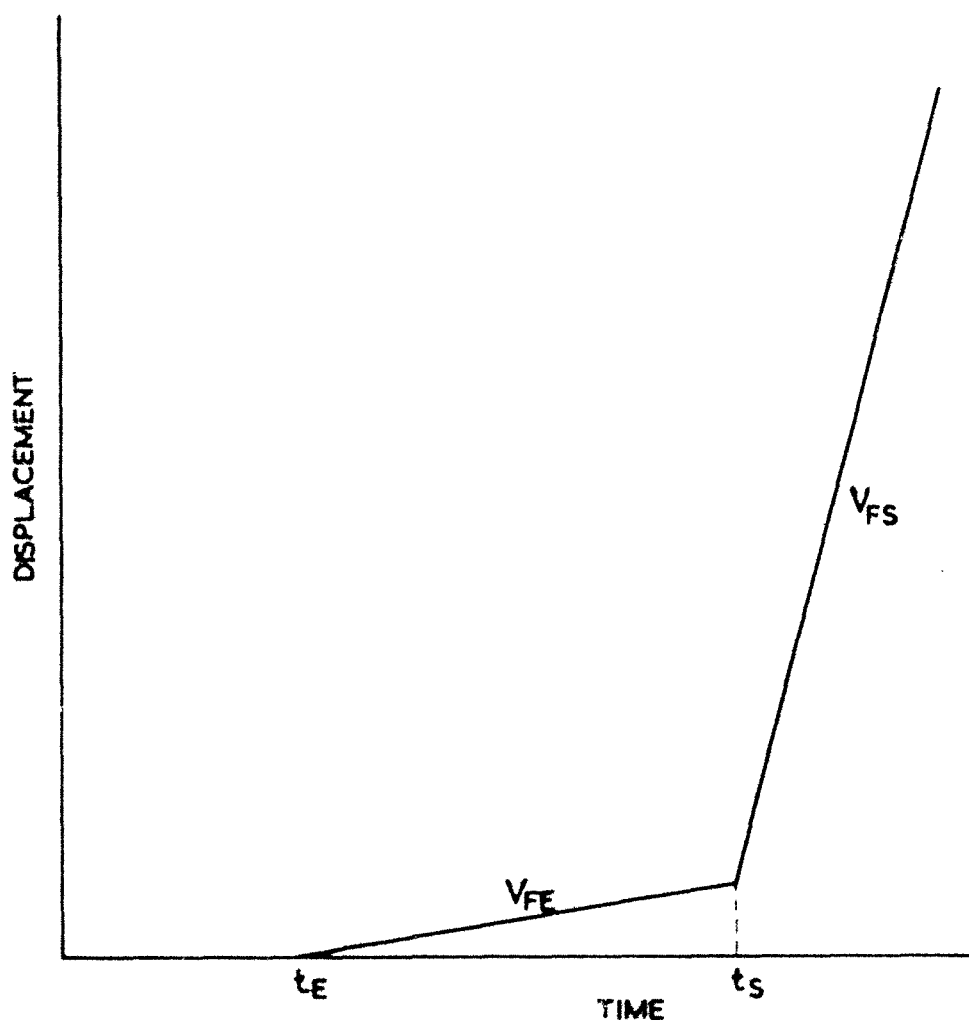


FIG. 24

SECRET

SECRET.

PRESSURE AT SHOCK - FRONT AGAINST
DISTANCE TRAVELLED.

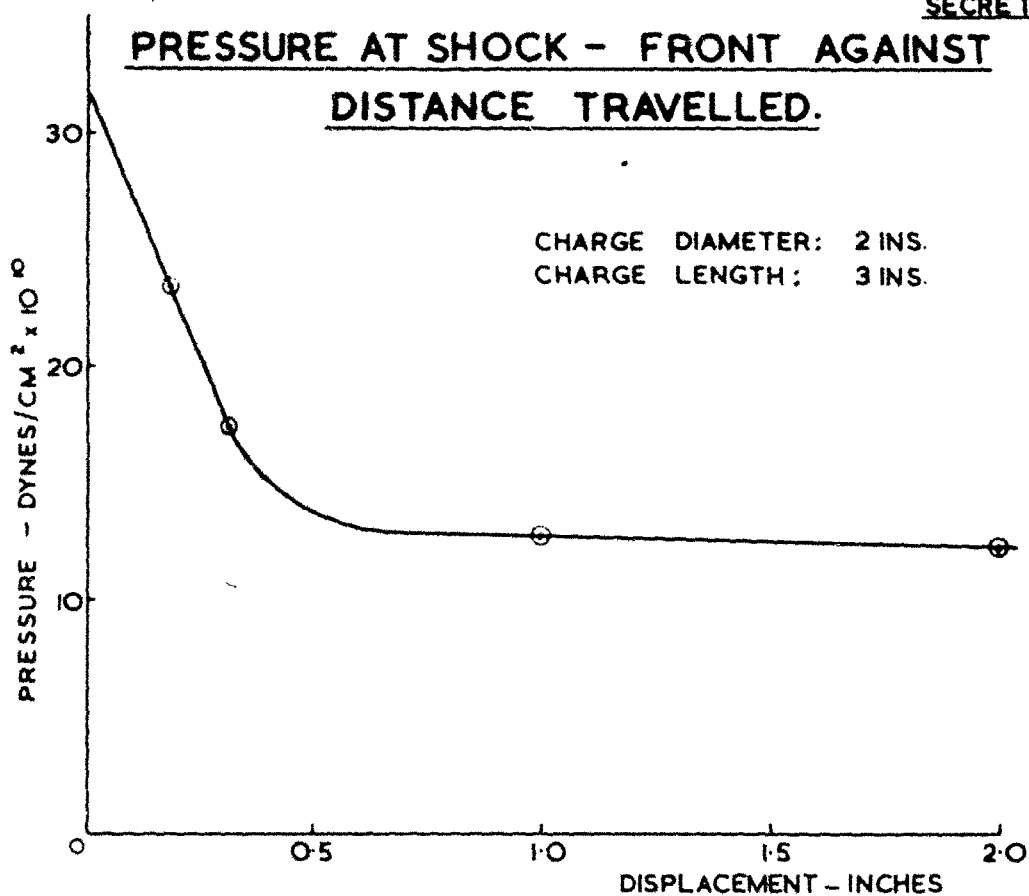


FIG. 25

PRESSURE - DISPLACEMENT CURVES AT
THREE DIFFERENT TIMES.

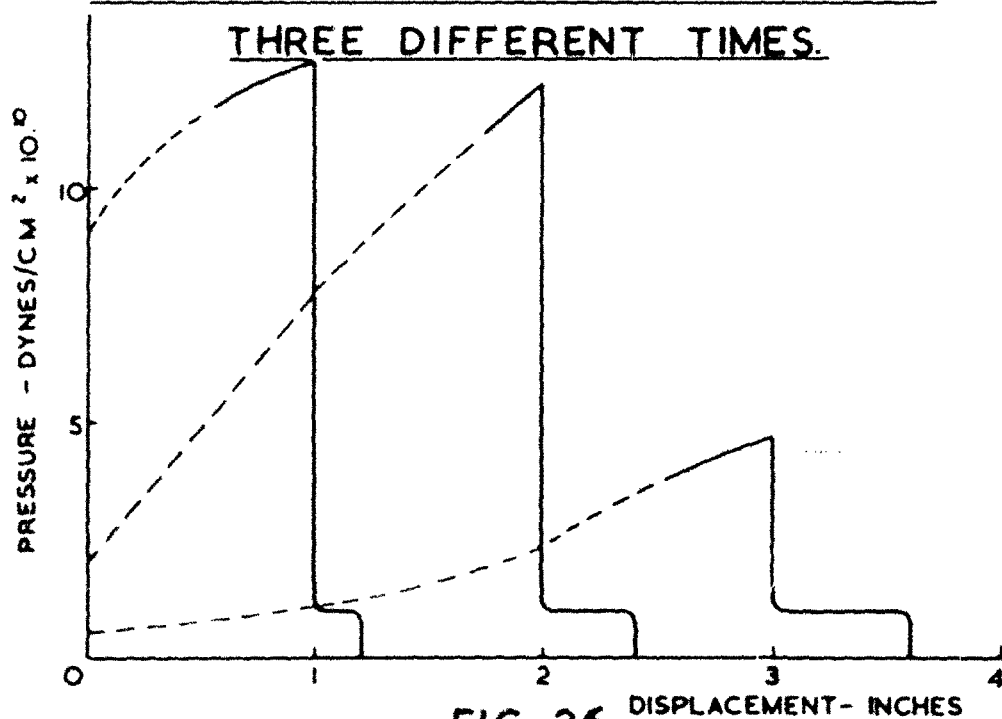


FIG. 26

SECRET.

SECRET

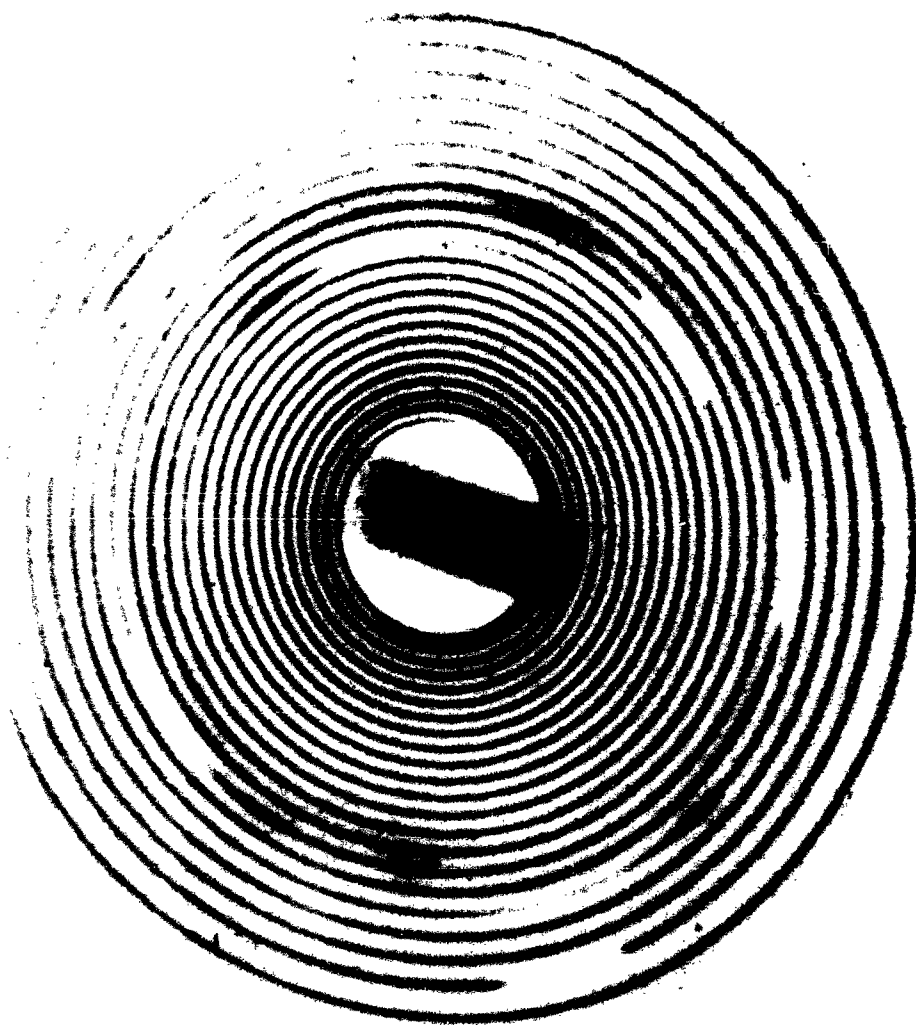
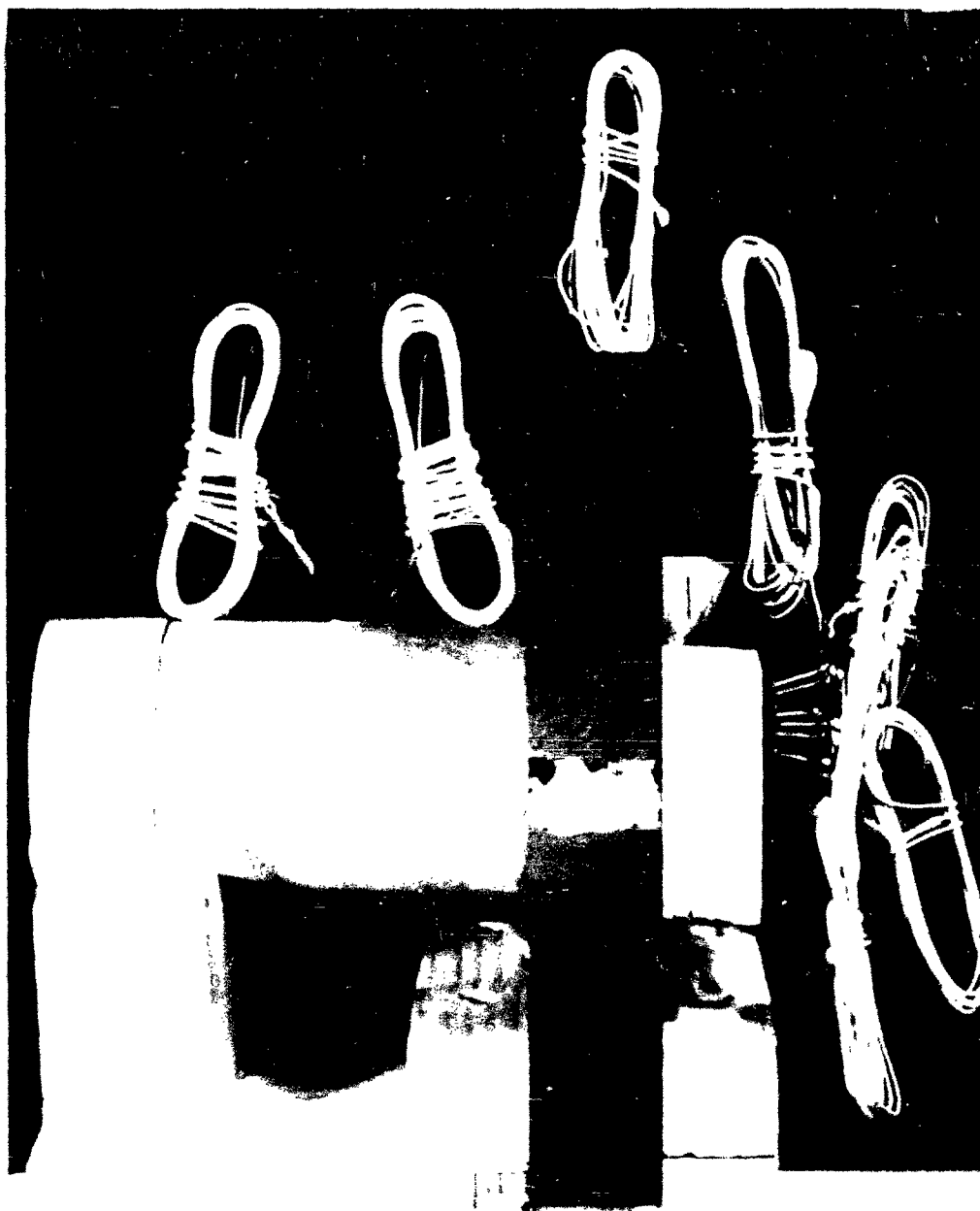


PLATE I. TYPICAL SPIRAL TRACE RECORD

SECRET



SECRET

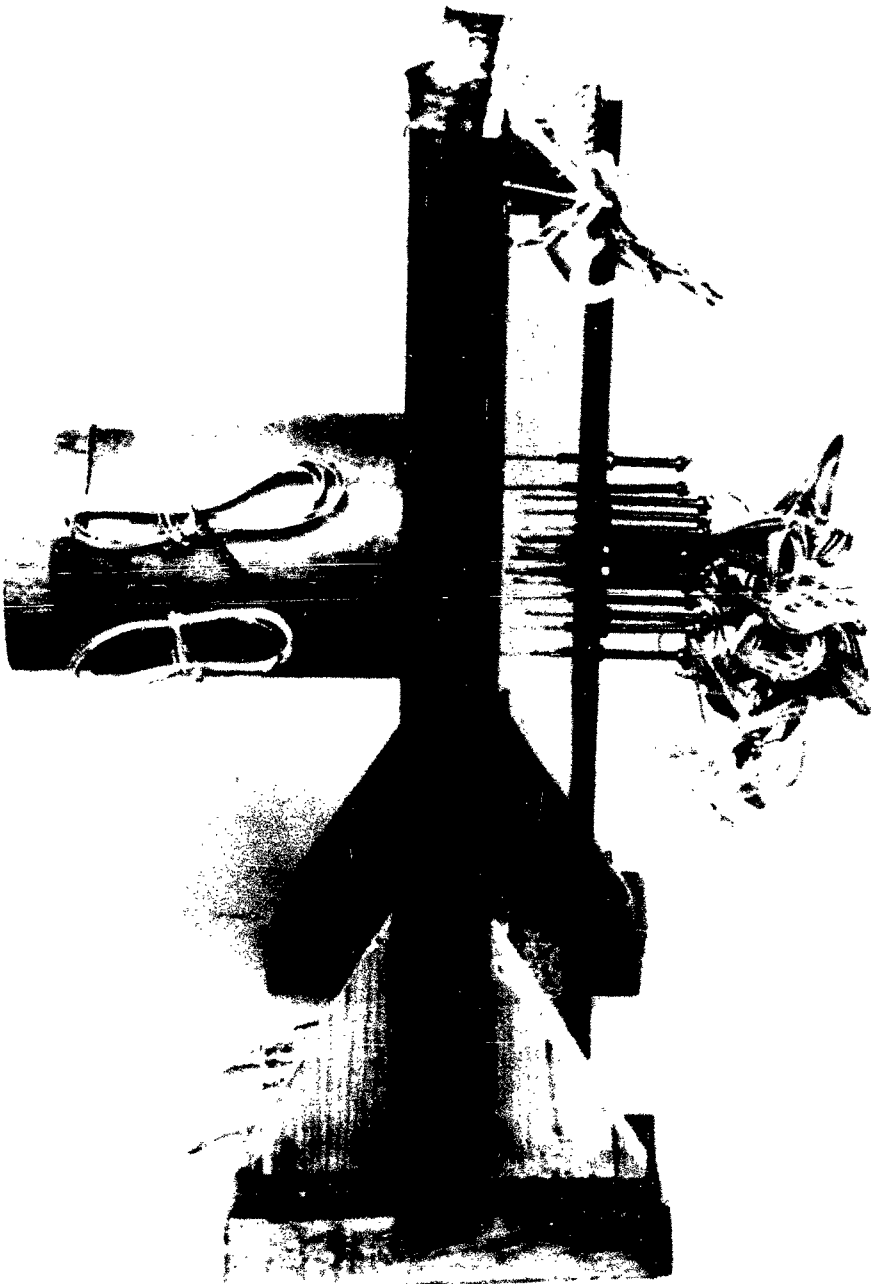


PLATE III CHARGE SET WITH THREE RINGS OF PROBES



*Information Centre
Knowledge Services*
[dstl] Porton Down,
Salisbury
Wiltshire
SP4 0JQ
22060-6218
Tel: 01980-613333
Fax 01980-613970

Defense Technical Information Center (DTIC)
8725 John J. Kingman Road, Suit 0944
Fort Belvoir, VA 22060-6218
U.S.A.

AD#: AD011687

Date of Search: 27 October 2008

Record Summary: DEFE 15/1818

Title: A Study of the Mechanism of Scabbing of Steel Plates by Explosive Attack
Availability Open Document, Open Description, Normal Closure before FOI Act: 30 years
Former reference (Department) Report 1/48 13/53
Held by The National Archives, Kew

This document is now available at the National Archives, Kew, Surrey, United Kingdom.

DTIC has checked the National Archives Catalogue website (<http://www.nationalarchives.gov.uk>) and found the document is available and releasable to the public.

Access to UK public records is governed by statute, namely the Public Records Act, 1958, and the Public Records Act, 1967.

The document has been released under the 30 year rule.

(The vast majority of records selected for permanent preservation are made available to the public when they are 30 years old. This is commonly referred to as the 30 year rule and was established by the Public Records Act of 1967).

This document may be treated as UNLIMITED.